
ABSTRACT

MOHAN, ANUSHREE Effect of Organic Solvent Exposure on Electret Filtration

(Under the direction of Dr. Warren J. Jasper)

The purpose of this research is to show that the electret filter media is affected by chemicals in the liquid phase. The work done by various other researchers validates the hypothesis that chemical vapors has little effect on the filter performance. But the existing methods of experimentation only show single phase results. The method described in this thesis represents a controlled approach to analyze the reduction of filtration efficiency when exposed to chemicals in both liquid as well as vapor phase.

The method clearly characterizes the flow and shows significant change in data to validate the experimental work done. This study does not consider the macroscopic or microscopic changes on the filter media. The research is primarily concerned with the loss of filtration efficiency due to chemicals.

The research provides a comprehensive, yet conclusive data on the effect of organic vapors on the electret filter media.

**EFFECT OF ORGANIC SOLVENT EXPOSURE ON
ELECTRET FILTRATION**

by

Anushree Mohan

A Thesis Submitted to the Graduate Faculty of
North Carolina State University
in Partial Fulfillment Of the Requirements for the Degree of
Master of Science

Textile Engineering

Raleigh

2005

APPROVED BY

Dr. Warren J. Jasper
Chair of the Advisory Committee

Dr. Roger L. Barker

Dr. Behnam Pourdeyhimi

Dedicated to

My Father the Beacon

My Mother the Pillar

My Brother the Madcap

BIOGRAPHY

Anushree Mohan, was born on December 31, 1981 in Pandalam, Kerala, India. She received a Bachelor of Technology in Textile Technology from Osmania University in 2003. She is currently pursuing a Master of Science in Textile Engineering at North Carolina State University. She is going to continue her Doctoral studies in Fiber and Polymer Science at North Carolina State University.

ACKNOWLEDGMENTS

I would like to express my sincere gratitude to my graduate advisor Dr. Warren J. Jasper for his constant support, guidance and motivation. A special thanks to Mr. Rob Grimes for all his guidance and patience. I take this opportunity to thank the T-PACC members for their help. I am grateful to NIOSH and Mr. Ken Williams for sponsoring this project.

Heartfelt thanks to my lab and research mates for their help and patient support.

Kudos to all my friends and roomies. You have just been through your worst nightmare!

Table of Contents

List of Figures	vii
List of Tables	x
1 Introduction	1
2 Literature Review	3
2.1 Respirator Filters	3
2.1.1 Mechanical Filter	3
2.1.2 Electret Filter	3
2.2 Charging Mechanisms	5
2.2.1 Tribocharging	5
2.2.2 Corona Charging	6
2.2.3 Electro-spinning	7
2.3 Particle Entrapment Mechanisms	7
2.3.1 Mechanical Filtration Mechanisms	8
2.3.2 Electrostatic Filtration Mechanism	9
2.3.3 Particle Capture by Electrostatic Mechanism	10
2.3.4 Mathematical Theory of Capture	12
2.4 Filter Performance	13
2.4.1 Filter Type	13
2.4.2 Filtration Efficiency	13
2.4.3 Aerosol Test Agents	14
2.4.4 Filter Test Data	14
2.4.5 Filter Loading	15
2.5 Evaluation of Filter Performance	15
2.5.1 Particle Charge and Size	16
2.5.2 Ambient Humidity and Temperature	16
2.5.3 Chemical Aerosols	17
2.6 Summary	17

3	Research Approach	19
3.1	Objectives	19
3.2	Approach	20
3.3	Instrumentation and Software	20
4	Experimental Work	22
4.1	Filter Media	22
4.1.1	Type of Charging Mechanism	22
4.1.2	Type of Filtration Efficiency	22
4.1.3	Packing Density	23
4.2	Baseline Test	23
4.2.1	Experimental Setup	23
4.3	Identification of Chemical Degradation	25
4.3.1	Liquid Immersion	25
4.3.2	Validation of Chemical Degradation	26
4.3.3	Chemical Exposure Apparatus	26
5	Results and Discussion	30
5.1	Baseline Tests	30
5.1.1	R and P Rated Filters	30
5.1.2	N Rated Filters	33
5.1.3	Tribo Charged Filters	35
5.1.4	Mechanical Filter	37
5.2	Investigation of Chemical Degradation	40
5.2.1	Liquid Immersion	40
5.2.2	Vapor Exposure	63
5.2.3	Toluene Exposure	64
5.2.4	Xylene Exposure	66
5.2.5	Ethyl Benzene Exposure	68
6	Conclusion	71
7	Appendix	73
7.1	Instrument Setup and Usage	73
7.2	Aerosol Generation	73
7.3	Aerosol Mixing and Transport	74
7.4	Particle Detectors	75
7.5	Microprocessor Control	75
7.6	Data Acquisition System	76
	List of References	81

List of Figures

2.1	Penetration of Aerosol through the Filter media [1]	4
2.2	Fiber Charge Configurations [2]	7
2.3	Particle Capture Mechanisms for a Filter Media [3]	8
2.4	Fractional Penetration Curves for Filter Media [4]	9
2.5	Filter Loading Behavior [5]	16
4.1	Experimental Setup for Chemical vapor exposure tests	28
5.1	Penetration Curve for the filter loaded with DOP	31
5.2	Resistance Curve for the filter loaded with DOP	31
5.3	Penetration Curve for the filter loaded with NaCl	32
5.4	Resistance Curve for the filter loaded with NaCl	32
5.5	Penetration Curve for the filter loaded with DOP	33
5.6	Resistance Curve for the filter loaded with NaCl	33
5.7	Penetration Curve for the filter loaded with NaCl	34
5.8	Resistance Curve for the filter loaded with NaCl	34
5.9	Penetration Curve for the filter loaded with DOP	35
5.10	Resistance Curve for the filter loaded with DOP	35
5.11	Penetration Curve for the filter loaded with NaCl	36
5.12	Resistance Curve for the filter loaded with NaCl	36
5.13	Penetration Curve for the filter loaded with DOP	37
5.14	Resistance Curve for the filter loaded with DOP	37
5.15	Penetration Curve for the filter loaded with NaCl	38
5.16	Resistance Curve for the filter loaded with NaCl	38
5.17	Penetration Curve for the filter immersed in Water	40
5.18	Resistance Curve for the filter immersed in Water	41
5.19	Penetration Curve for the filter immersed in Water	42
5.20	Resistance Curve for the filter immersed in Water	42
5.21	Penetration Curve for the filter immersed in Water	43
5.22	Resistance Curve for the filter immersed in Water	43
5.23	Penetration Curve for the filter immersed in Water	44
5.24	Resistance Curve for the filter immersed in Water	44
5.25	Penetration Curve for the filter immersed in Acetone	46

5.26	Resistance Curve for the filter immersed in Acetone	46
5.27	Penetration Curve for the filter immersed in Acetone	47
5.28	Resistance Curve for the filter immersed in Acetone	47
5.29	Penetration Curve for the filter immersed in Acetone	48
5.30	Resistance Curve for the filter immersed in Acetone	48
5.31	Penetration Curve for the filter immersed in Acetone	49
5.32	Resistance Curve for the filter immersed in Acetone	49
5.33	Penetration Curve for the filter immersed in Methyl Ethyl Ketone . .	51
5.34	Resistance Curve for the filter immersed in Methyl Ethyl Ketone . . .	51
5.35	Penetration Curve for the filter immersed in Methyl Ethyl Ketone . .	52
5.36	Resistance Curve for the filter immersed in Methyl Ethyl Ketone . . .	52
5.37	Penetration Curve for the filter immersed in Methyl Ethyl Ketone . .	53
5.38	Resistance Curve for the filter immersed in Methyl Ethyl Ketone . . .	53
5.39	Resistance Curve for the filter immersed in Methyl Ethyl Ketone . . .	54
5.40	Resistance Curve for the filter immersed in Methyl Ethyl Ketone . . .	54
5.41	Penetration Curve for the filter immersed in Hexane	55
5.42	Resistance Curve for the filter immersed in Hexane	55
5.43	Penetration Curve for the filter immersed in Hexane	56
5.44	Resistance Curve for the filter immersed in Hexane	56
5.45	Penetration Curve for the filter immersed in Hexane	57
5.46	Resistance Curve for the filter immersed in Acetone	57
5.47	Resistance Curve for the filter immersed in Hexane	58
5.48	Resistance Curve for the filter immersed in Hexane	58
5.49	Penetration Curve for the filter immersed in Toluene	59
5.50	Resistance Curve for the filter immersed in Toluene	59
5.51	Penetration Curve for the filter immersed in Toluene	60
5.52	Resistance Curve for the filter immersed in Toluene	60
5.53	Penetration Curve for the filter immersed in Toluene	61
5.54	Resistance Curve for the filter immersed in Toluene	61
5.55	Resistance Curve for the filter immersed in Toluene	62
5.56	Resistance Curve for the filter immersed in Toluene	62
5.57	Penetration Curve for the filter exposed to Toluene	64
5.58	Penetration Curve for the filter exposed to Toluene	64
5.59	Penetration Curve for the filter exposed to Toluene	65
5.60	Penetration Curve for the filter exposed to Toluene	65
5.61	Penetration Curve for the filter exposed to Xylene	66
5.62	Penetration Curve for the filter exposed to Xylene	66
5.63	Penetration Curve for the filter exposed to Xylene	67
5.64	Penetration Curve for the filter exposed to Xylene	67
5.65	Penetration Curve for the filter exposed to Ethyl Benzene	68
5.66	Penetration Curve for the filter exposed to Ethyl Benzene	68
5.67	Penetration Curve for the filter exposed to Ethyl Benzene	69

5.68	Penetration Curve for the filter exposed to Ethyl Benzene	69
7.1	Schematic Diagram of Automated Filter Tester	74
7.2	Block Diagram-Data Collection Database	77
7.3	Database I/O Window	78
7.4	Search Window in the Database	79
7.5	Data Assimilation and Analysis	79
7.6	Database Capabilities	80

List of Tables

2.1	Triboelectric series of Fibers [1]	6
4.1	Filter Media Specifications	24

Chapter 1

Introduction

Electrets are electrically charged filter media used in respirator masks. This advancement was a major achievement in respiratory protection as these filters improved the efficiency at the most penetrating particle size while cutting down the pressure drop to half. Hanson [?] developed the first electrostatically charged filter. Initially, glass fibers were used to manufacture non-woven media used in respirator masks. The mechanical filters worked as a sieve to filter out particulates which thereby resulted in the formation of cake over the filter surface. This increased the pressure drop, and made it difficult for the wearer to breathe. The basic principles involved in the filtration process with mechanical filters is interception and impaction, for large particles and diffusion for smaller particles.

The electret filters work with electrostatic filtration as the principal form of filtration in the most penetrating particle size range of $0.1\mu\text{m}$ - $0.3\mu\text{m}$ [6]. The charge on the fibers improves the efficiency of the filters, hence a lower fiber density is sufficient to obtain up to 99% filter efficiency. The lower fiber density reduces the pressure drop tremendously.

Electrets are permanently polarized dielectrics. Three of the most common methods of electrostatic charging of filter media are corona charging, tribocharging and electro-spinning. Synthetic polymers with low conductivity are used for the manufacture of respiratory filter media as they are suitable for charge retention. Initially the electrostatic filter media was manufactured by triboelectric exchange where two different types of fibers were carded together, resulting in the generation of charge

on the fiber surface. Later, various types of corona charging methods were developed wherein a permanent dipole moment was imbedded on the surface.

The principle behind the charging mechanism is that, when an electric field is applied to a polymer above its glass transition temperature, (T_g), the molecules align themselves in the direction of the electric field. On solidifying, the molecules are no longer mobile and keep their orientation which results in permanent electric polarization. As a result of polarization, the molecules will have electric charges whose surface density is numerically equal to the electric moment per unit volume. The neutralizing the effect of this charge movement, the media appears non electrified. It is also assumed that the molecules of the substance are permanently polarized and the amount of polarization depends upon the temperature.

These electrically charged filters appear to be stable under normal conditions for a long duration of time. The focus of this research is to study the influence of organic solvents on the filtration performance of electret filter media. An extensive literature survey and substantial experimental work was done to set base for a controlled experimental setup. The filter media were exposed to organic vapors in liquid as well as vapor phase. The hypothesis for this work is that organic solvents cause decrease in filter efficiency in electrets in the liquid phase as a diffusion rate limited process.

Chapter 2

Literature Review

2.1 Respirator Filters

The critical concern in respiratory protection is associated with particles that have aerodynamic diameters less than $2\mu\text{m}$. These particles can reach the respiratory tracts and settle down in the tracts of the human body [7, 8].

Two types of filter media are generally used:

- Mechanical filters
- Electrostatically charged filters (Electrets).

2.1.1 Mechanical Filter

Mechanical filters can be produced from micro-sized glass fibers. However, these filters have the disadvantage of high pressure drop across the filter and greater energy expenditure. An increase in pressure drop is also observed due to caking of accumulated particles. [9]

2.1.2 Electret Filter

Since the mechanical filter shows high resistance, the electret filter media is a better choice for respiratory masks [10]. Fibers with low conductivity were charged and they could retain their charge for a long period of time. These fibers were then used in the manufacture of respirator filter media [11]. The electrical forces are beneficial in the

capture of both charged and neutral particles. A charged fiber attracts an oppositely charged particle by Coulombic forces, and a neutral particle by polarization forces [12, 6].

A relative comparison of filtration between a mechanical filter and an electret filter can be seen in Figure 2.1.

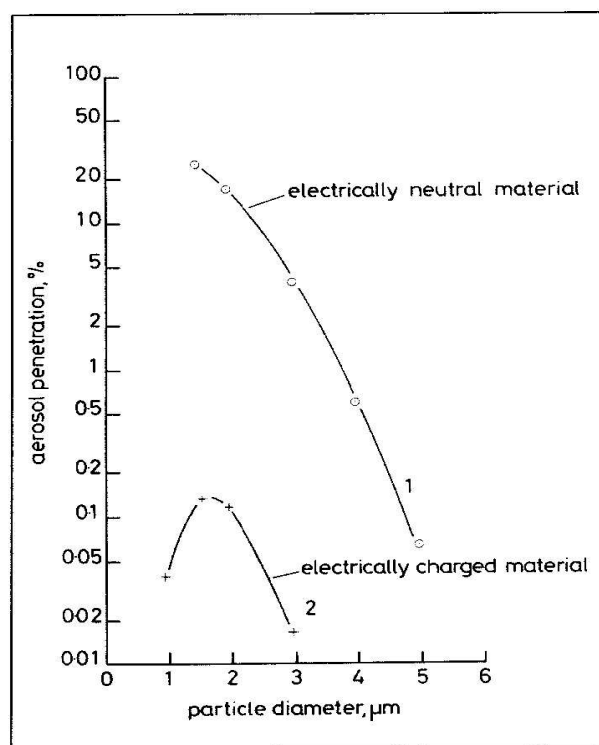


Figure 2.1: Penetration of Aerosol through the Filter media [1]

As seen from the above figure, the electric charge increases the filtration efficiency considerably. The high capture efficiency applies to both charged and neutral particles. Charged particles are captured by Coulombic forces while the neutral particles due to their polarisability [11]. As stated by Brown [1], the electric field produced by a charged particle polarizes a neutral particle and the component of the dipole that is nearer to the fiber will be in a region of higher electric field than its counterpart. So it will experience an attractive force slightly higher than the repulsive force acting on the other. This slight imbalance results in an attractive force on the particle. The

magnitude of the force is proportional to the size of the particle.

2.2 Charging Mechanisms

Following are the various methods used to charge these filter media:

1. Tribo-Charging
2. Corona Charging
3. Electro-Spinning

2.2.1 Tribocharging

This was the first process of charge induction in filters. This phenomenon occurs when two different types of fibers with dissimilar electrical properties are carded together. When the fibers are combed out into an open structure, the triboelectric exchange (generation of static electric charge) causes the fibers to charge. Usually a highly electropositive material is blended with a highly electronegative material. The fibers have diameters in the range of $20 - 100\mu m$. The non-woven media is usually needlepunched, hence is bulkier and has low pressure drop [1, 13]. Different fibers used in triboelectric charging have been listed in Table 2.1.

Hanson [14] invented the first triboelectric filter media by mixing wool with resin. During carding, the resin fibers charge negatively and wool attains positive charge therein creating a balance in charge and nullifying the overall charge on the filter media. This phenomenon helps in better charge retention as the charge is not on the surface of the filter media but entrapped within. The charge stability is due to the low conductivity of resin, while the relatively conducting wool fibers develop image charges. The most commonly manufactured triboelectric filter media comprises of polypropylene fibers and chlorinated polymer fibers. Polypropylene which acquires positive charge is responsible for the charge stability [15].

Positive	Wool Nylon66 Nylon6 Silk Regenerated Cellulose Cotton Polyvinyl Alcohol Chlorinated Wool Cellulose Triacetate Acrylic Polytetrafluoroethylene Polyethylene Polypropylene Poly(ethylene terephthalate) Poly(butylenes terephthalate) Modacrylic
Negative	Chlorofiber

Table 2.1: Triboelectric series of Fibers [1]

2.2.2 Corona Charging

A thin sheet of polymer is placed on a conducting surface and a point electrode is emits ions at a very high potential. The ions from this electrode will drift under the influence of the field to a lower potential (polymer sheet). If the sheet is insulating, charge will develop [16]. The sheet is then stripped from its conductive backing and an opposite charge is generated, giving rise to sheet dipole configuration. This configuration can also be produced with two electrodes of opposite charges. When such a sheet is stretched longitudinally, molecular realignment occurs and causes the sheet to fibrillate. This results in a line dipole configuration of charge. The fiber has a rectangular cross-section and is stronger in the direction of stretching and weaker in the direction perpendicular to it. The fibers are then carded in to a filter web [10, 17, 2].

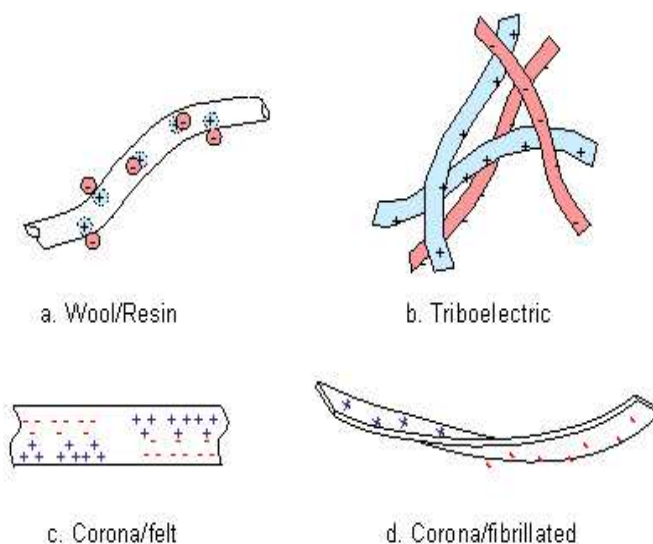


Figure 2.2: Fiber Charge Configurations [2]

2.2.3 Electro-spinning

A conductor in an electric field will develop a surface charge which reduces its internal field to zero. The charge thus developed is dipolar. This is the behavior shown by small droplets produced by electrostatic spraying. A polymer melt will delay its breaking into droplets and the liquid filament will solidify into a fiber. Electrostatically extruded fibers have diameters as low as $1 - 2\mu\text{m}$.

2.3 Particle Entrapment Mechanisms

Filtration in electret filters is achieved by various particle capture mechanisms such as:

1. Gravitational Settling
2. Interception
3. Impaction
4. Electrostatic attraction

5. Brownian Diffusion

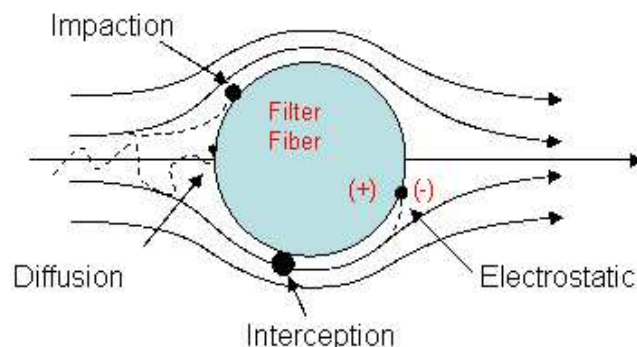


Figure 2.3: Particle Capture Mechanisms for a Filter Media [3]

2.3.1 Mechanical Filtration Mechanisms

Gravitational settling is not an important mechanism as it only involves large particles that settle onto the filter due to gravity. Particle interception and impaction are basically mechanical filtration mechanisms. In interception, the particle is intercepted by the filter when its flow stream comes within a close proximity of the fiber. It is nothing but a physical interference between the particles and the fibers. While inertial impaction occurs when a particle deviates from its flow stream and impacts onto the fiber. Both these mechanisms are prominent in the capture of micrometer sized particles. Aerosol particles captured by these mechanisms usually deposit on the surface of the fibers. Diffusion is a random Brownian motion of submicro sized particles caused from collisions with molecules [9, 3, 18].

The curve shown in Figure 2.4 demonstrates the general penetration behavior with the combined effects of diffusion, interception and impaction. The shape of the curve and the magnitude of penetration will depend on the filter media characteristics and the airflow velocity. The most penetrating particle size (MPPS), as shown, is a function of the charge state of the filter media and the particle size between 0.1 –

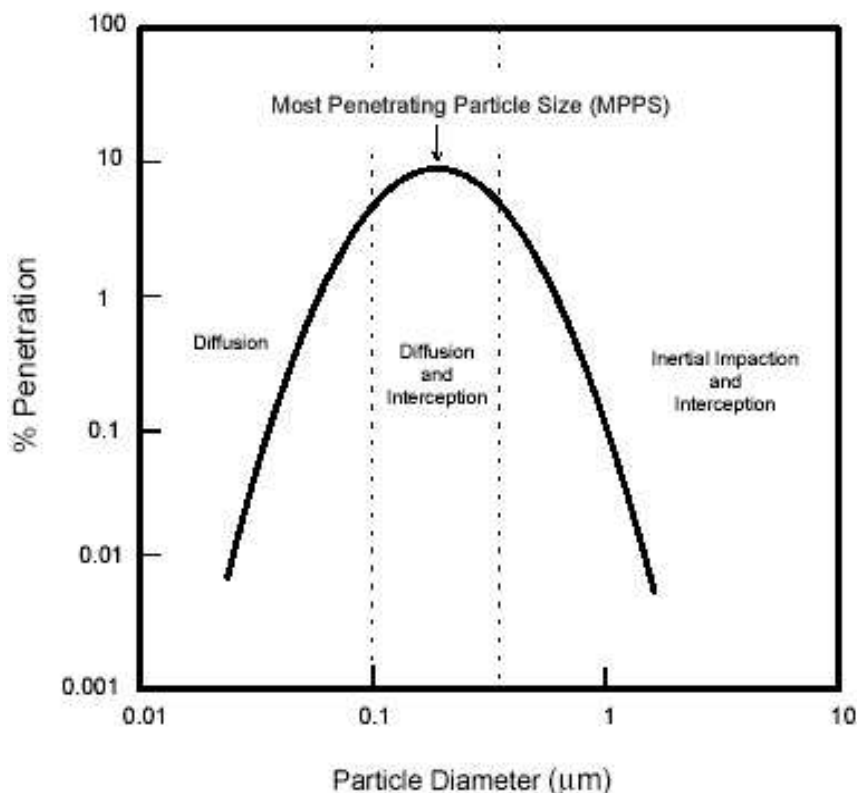


Figure 2.4: Fractional Penetration Curves for Filter Media [4]

$0.3\mu m$. The charged particles seemed to be in the $0.3\mu m$ range while the neutral particles were nearer to $0.1\mu m$ [4, 19].

2.3.2 Electrostatic Filtration Mechanism

The mechanism of concern in this research is electrostatic filtration. Walsh [?] suggests that if a particle is collected by inertia or interception, then it can only be deposited on the front of the fiber. If it is collected by electrostatics then it is also deposited in the rear. This helps in efficiently using the space within the fiber and hence the clogging point is increased [?]. It works on the principle of electrical attraction between the permanently charged regions of a filter fiber and aerosols, either charged or uncharged. These filters have high microscopic charge and a low macroscopic charge; hence the field effects are only apparent near the surface of the

fiber. [18] Most of the theory behind particle capture mechanisms assumes that the fiber is a single uniformly charged cylinder. The mean air speed perpendicular to the fiber is U [20, 21].

As derived by the electrostatic theory the electric field \mathbf{E} , at a distance r perpendicular to an infinite rod, is given by

$$\mathbf{E} = \frac{Q}{2\pi\epsilon_0\mathbf{r}} \quad (2.1)$$

where Q is the charge per unit length and ϵ_0 is the permittivity of free space with value $\frac{10^{-9}}{36\pi}$ Farads/meter. As we know the force acting on a particle with charge q is given by:

$$\mathbf{F} = \mathbf{E} \times q \quad (2.2)$$

As a particle moves through a fluid, it will attain a drift velocity which is nothing but the product of the force acting on the particle and its mechanical mobility μ given by:

$$\mu = \frac{C_n}{3\pi\eta d_p} \quad (2.3)$$

where C_n is the Cunningham correction factor. The Cunningham factor approaches unity for particles larger than the mean free path of air, and thus can be ignored. As the diameter increases, the aerodynamic slip increases particle mobility [12].

For mechanical filters, μ physically is the constant of proportionality between the coefficient of diffusion and the average thermal energy, k_bT . The ratio of the drift velocity toward the fiber to the free stream velocity at the fiber surface is given by:

$$N_{Qq} = \frac{V_d}{U} = \frac{Qq}{3\pi^2\epsilon_0\eta d_p d_f U} \quad (2.4)$$

2.3.3 Particle Capture by Electrostatic Mechanism

The two important factors that determine particle capture by electric forces are charge strength and its distribution on the fibers, and charge distribution on the particles.

Brown looks at three different cases of electric charge distributions on aerosol particles:

- Breakdown charge distributions
- Equilibrium charge distributions
- Miscellaneous charge distributions

The voltage at which air conducts electricity is approximately 3×10^6 V/m. If the particle is assumed to be a point charge, then the amount of charge in Coulombs at a distance of the radius of the particle becomes:

$$q_{\text{breakdown}} = 8.33 \times 10^{-17} d_f \quad (2.5)$$

where d_f is the diameter of the fiber in micrometers. If the electrostatic energy of the particles were equivalent to the average kinetic energy due to Brownian motion, the Boltzmann charge distribution would be:

$$\frac{\langle q^2 \rangle}{4\pi\epsilon_0 d_p} = \frac{1}{2} k_b T \quad (2.6)$$

Where T is in degrees Kelvin and k_b is the Boltzmann's constant. Here, the charge q would have a Gaussian distribution, with a mean value of $q_{\text{mean}} = 3.84 \times 10^{-19} d_p^{0.5}$. It can be seen from above that the charge on the particle from a Boltzmann distribution is 2 orders of magnitude smaller than the breakdown voltage. But this charge value seems unreasonable for small particles, hence an approximation is that a fraction of particles hold unit charge while the rest are neutrally charged.

Capture of neutral particles

An electric field can influence a neutral particle by polarizing it and inducing a dipole. It is this dipole that gets attracted to the fiber electrostatically. The magnitude of the electric dipole is proportional to the electric field at a position of the particle and to the particle volume, and it also depends on the dielectric constant of the material making up the particle. The electric field due to the charged fiber falls off with increasing distance, and so one part of the dipole will be more strongly attracted to the fiber than the repelled part. This results in a net imbalance and an attractive force given as:

$$F_r = \frac{\pi d_p^3 \varepsilon_0}{4} \left(\frac{D_p - 1}{D_p + 2} \right) \nabla (E^2) \quad (2.7)$$

As seen in the above equation, the force depends upon the field gradient and not the field itself. But a uniform field would produce no net force on a neutral particle as the force acting on the dipole would have the same magnitude but opposite sign. For a uniformly charged fiber the equation becomes:

$$F_r = \frac{Q^2 d_p^3}{8\pi \varepsilon_0 r^3} \left(\frac{D_p - 1}{D_p + 2} \right) \quad (2.8)$$

Hence the dimensionless parameter N_Q , that describes the capture efficiency for a neutral particle can derived as:

$$N_Q = \frac{Q^2 d_p^2 C_n}{3\pi^2 \varepsilon_0 \eta d_f^3 U} \left(\frac{D_p - 1}{D_p + 2} \right) \quad (2.9)$$

2.3.4 Mathematical Theory of Capture

Brown describes three methods to calculate capture efficiency:

Capture of particle by solenoidal forces

A solenoidal vector field is one whose divergence is zero. i.e., $(\nabla \cdot E = 0)$. But this theory does not hold good for a fiber as a fiber is not a point charge but a long cylinder.

Capture by central forces

This model can be applied for both coulomb forces and polarization forces, if it is clear that the fiber is uniformly charged throughout. The differential form of the function looks like:

$$d\psi = \frac{\partial \psi}{\partial r} dr + \frac{\partial \psi}{\partial \theta} d\theta \quad (2.10)$$

Here the first term is related to the tangential velocity and the second to the radial velocity. If no external forces act on the particle, then it remains in the stream line

with $d\psi = 0$. If a central force $F_r(r)$ acts on the particle with a mobility factor μ , the change in the stream function becomes:

$$d\psi = r\mu F_r(r)d\theta \quad (2.11)$$

These differential methods should be solved numerically by iterative methods such as Runge-Kutta or Adams-Bashforth. Hence it can be concluded that the parameters that influence the particle capture mechanism are charge, charge distribution, particle size and fiber size.

2.4 Filter Performance

NIOSH (National Institute for Occupational Safety and Health) has specified a standard testing procedure to certify these filters and filter media. The certification standard particulate filtration is in 42 CFR part 84.

According to 42 CFR part 84 there are two ways to classify these filters:

- According to the Filter type
- According to the Filtration efficiency

2.4.1 Filter Type

According to the 42 CFR part 84, there are three different types or grades of filters - N, R and P. The N rated filters are tested only with solid aerosol particles; these filters are not resistant to oil. The R rated filter is resistant to oil and is tested with both liquid and solid aerosol particles. The P rated filters are also tested with both liquid and solid aerosols [22].

2.4.2 Filtration Efficiency

These three types of filters are segregated into three levels of filter efficiency - 95,99 and 99.97%. Each filter tested is then given specific use for different environments.

2.4.3 Aerosol Test Agents

Two test agents standardized by NIOSH as test agents to represent the solid and liquid aerosols are NaCl (Salt) and DOP (Di-Octyl Pthalate). Two different types of aerosol generators are used to generate aerosols for the tests. These generators are capable of generating particles in the size range of $0.1\mu\text{m}$ - $0.5\mu\text{m}$. This is the size range for particles captured by diffusion and electrostatic mechanism. The salt aerosol generator releases aerosol with Count Median particle Diameter (CMD) of $0.075\mu\text{m}$, and a Mass Median diameter (MMD) of $0.26\mu\text{m}$ and geometric standard deviation of 1.5. The DOP aerosol with a count median particle diameter (CMD) of $0.2\mu\text{m}$, a Mass Median particle diameter of $0.33\mu\text{m}$ and a geometric standard deviation of 1.6. Salt is highly ionic, therefore an ionizer is used to ionized air molecules and mix them with salt aerosol. The interaction between these two results in the overall charge of the aerosol to be neutral.

2.4.4 Filter Test Data

The TSI 8130 filter tester is used to test these filters at a constant rate of flow specific to the end use of the filter. The aerosol percent penetration and pressure drop (mm of H_2O) across the filter media is obtained from the tester. Both these values are used to determine the efficiency of the filter media. The difficulty in correlating penetration values between two different types has always been a problem. Brown developed a method to normalize the penetration values between filter types so that their performance could be compared.

$$\text{NormalizedPenetration} = e^{\left(\frac{\text{StandardWeight}}{\text{ActualWeight}} \times \ln \text{MeasuredPenetration}\right)} \quad (2.12)$$

Another method to compare filter performance would be in terms of Quality Factor [23, 7].

$$\text{QualityFactor}(QF) = \frac{\ln(100/P)}{\Delta p} \quad (2.13)$$

Where P is Percent Penetration

Δp = Pressure drop in MM of H₂O

2.4.5 Filter Loading

Figure 2.5 illustrates a typical loading behavior of an electret filter media. The filter was loaded with 1.03 μ m stearic acid aerosol particles at 0.1m/s. The penetration through the filter increases initially as the charge on the filters is reduced by the depositing particles. Once the maximum penetration is reached, the filter efficiency starts increasing as the electret filter starts behaving like a mechanical filter due to particle caking [24]. The caking of deposited particles on the filter surface restricts the influence of charges on filtration performance of the media. The particles form a dendritic structure on the filter surface. Brown believes that the charge is screened by the captured particles, which depends on its covering capability. According to Brown [25], a thin film of small particles will prove to be an effective screen than a few large particles. The pressure drop increases as the filter gets clogged by particles. Walsh defines the clogging point as the mass deposited at which as line extrapolated from the second linear portion of the pressure versus loading curve intersects the mass deposited axis. Such a behavior is not observed with liquid particles as liquid particles spread over the filter media and diffuse through the interstices [26, 5]. The filter performance against liquid aerosol starts out high and then reduces as more and more particles are passed through. The resistance or pressure drop does not change throughout the loading process.

2.5 Evaluation of Filter Performance

In order to evaluate the filter performance, we must understand what causes the reduction of filter performance. Extensive study has been done to understand the effect of particle size, particle charge, type of particle, temperature, humidity, chemicals and storage time.

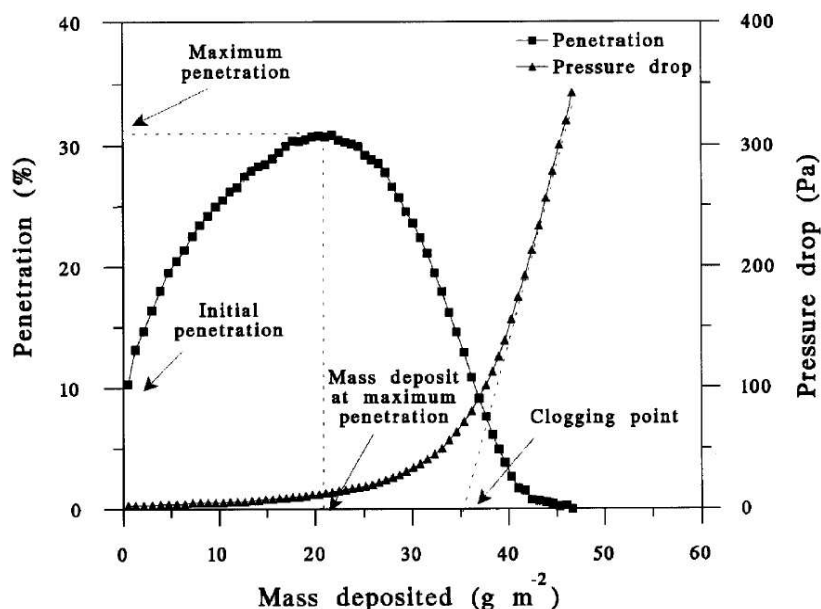


Figure 2.5: Filter Loading Behavior [5]

2.5.1 Particle Charge and Size

The influence of the particles was studied by spray electrifying them so that they hold a higher charge. It was seen that the highly charged particles were captured at the initial stages of particle capture. Also the filter efficiency for these particles was high when compared to equilibrium charged particles. It has also been shown that the smaller the particles, the quicker the loading, the higher is the reduction in electrostatic capture. Another point to be noted is that liquid particles cause a higher reduction in filter efficiency than solid particles [5, 27].

2.5.2 Ambient Humidity and Temperature

All the study done so far indicates that the electric charge on the filter is quite stable and does not reduce due to storage environment, unless the fibers used for the manufacture of the filter media are susceptible to moisture [28, 29, 30].

2.5.3 Chemical Aerosols

Exposure to chemical challenge agents has always been an interesting topic. Respiratory handbook [14] lists a series of tests done by Biermannman, wherein the filter media is immersed in different solutions like water, water and nitric acid, water and surfactant and water plus surfactant and salt [31]. These filters were immersed in the solutions for 30 minutes and then allowed to dry. The filtration efficiency reduced by 60% when immersed in water plus surfactant and salt due to the ionic interaction of salt. The filters are generally manufactured from hydrophobic fibers to reduce the effect of humidity during storage. This property of the fiber does not allow water to wet the filter surface, hence no significant deterioration occurred when immersed in water. The filter media was also immersed in various organic solvents such as Heptane, Isooctane, Cyclohexane, Benzene, Toluene, Acetone, Methyl Ethyl Ketone. All these solvents decreased the filtration efficiency but the mixture made from these solvents had a stronger impact. Organic solvents dissolve the filter surface hence affect the fiber charge.

When the filter was immersed in isopropanol, the filter efficiency significantly decreased, while no significant difference was observed in the pressure drop. This however helps us understand that these solvents dissipate the charge on the fiber surface without changing the physical properties of the fiber. All the above test results cannot be used to predict the electrostatic behavior of the filter media as immersion in liquid solvents is not what these filters are manufactured for. These tests can be considered as an extreme case of exposure to chemical solvents. The filters were then exposed to chemical aerosols for 8 hours at TLV, which represents a normal work place exposure limit. A decrease in the filtration was observed but this was significantly lower than that observed from liquid solvents [30, 32, 31].

2.6 Summary

The review of literature suggests a need to understand the electrostatic filtration mechanism. It gives an in depth understanding of clogging of large, and submicro

sized particles onto the filter media. It also gives a descriptive evidence of the influence of the particles on the charge on the filter media. Mathematical evidence has also been given for the clogging and capture mechanisms of particles. Workplace studies have been conducted to study the filtration efficiency of these filters in standard workplace conditions. All the above work shows that these filter are highly efficient for solid and liquid particles even in the most penetrating particle size. The degradation mechanisms of these filters had also been widely investigated. The literature suggests that the hazardous vapors do not cause any dissipation of charge. It also throws light on the study with liquid solvents. The study shows that filtration performance reduces with immersion in to liquid solvent.

But all the work done is specific to one phase, results. No study clearly defines a comparison of the two phase (Liquid and Solid) results.

Chapter 3

Research Approach

How does the electrostatic filtration mechanism work? What causes the particles to be held onto the filter media? How long do these charges stay on the filter surface? Is charge retention a microscopic or a macroscopic property? Is the charge screened or destroyed or neutralized, or does it just dissipate from the surface? What causes the filtration efficiency to degrade? How does a filter load particles onto the surface and into the interstices? These are a few questions that have been dealt with in most of the papers. The process of charge capture and retention by the fiber, the influence of aerosol type and the significant degradation of the filter media due to exposure to liquid solvents or vapors are various areas of research that could be worked further on. How does the filter media perform when stored in ambient laboratory environment? What change in filtration efficiency is observed when brought in contact with industrial chemicals? How does the electret performance deteriorate when exposed to organic solvent?

This research aims to show that exposure to organic solvents in liquid phase can cause a decrease in filter efficiency. It has already been proved that organic vapors do not affect the static charge on the filters.

3.1 Objectives

The main objective of this study is to identify various conditions that can result in the decrease of filtration efficiency. This was achieved in the following ways:

1. Assimilate the general filter efficiency data.
2. Observe the effect of organic vapor on the filter media.
3. Analyze the influence of liquid solvents.
4. Validate the effect of liquid organic solvents on the filter efficiency.

3.2 Approach

There were three main parts in this study. The first part was to understand the general filter media specifications. To accomplish that, general baseline tests were conducted with standard test agents DOP (Di-Octyl Phthalate) and NaCl. In the second part, various tests were conducted to determine the conditions that cause a reduction in filter efficiency. This was achieved by exposing the filters to organic vapors as well as immersing them in liquid solvents. The third and final set of experimentation was to confirm the influence of solvent phase on filter efficiency. A controlled experimental setup was devised to observe this effect.

3.3 Instrumentation and Software

A CertiTest 8130 automated particulate filter tester was used to determine the performance (percentage penetration) and resistance (pressure drop in mm of H₂O) of the filter media. The CertiTest® 8130, manufactured by TSI Incorporated in St. Paul, MN, is equipped with oil and salt aerosol generators. DOP was used as a standard test agent in the oil aerosol generator to produce particles with a count median diameter of $0.20\mu\text{m}$ and a geometric standard deviation of less than 1.6. Sodium Chloride was used in the salt generator to produce solid aerosol particles with a count median diameter of $0.075\mu\text{m}$ and a geometric standard deviation of less than 1.8. The filter media were tested as flat samples, using a constant surface area of 6 inch diameter face area. All the tests were done according to the criteria established in 42 CFR 84 for challenging respirator filter media.

A gas chromatograph (GC-17A Shimadzu Instruments, Columbia MD) equipped with a 30m capillary column, 0.53mm ID (Stabilwax® crossbond® carbowax®-PEG) and a flame ionization detector was used to determine the concentration of chemical in the gas entering and leaving the exposure apparatus. The method was calibrated using calibrated mixtures certified by The Specialty Gas Group (Raleigh, NC).

Chapter 4

Experimental Work

4.1 Filter Media

The filter media was selected such that all the different types of filter media could be tested and understood. The media was selected based on the:

- Type of Charging Mechanism
- Type of Filtration Efficiency
- Packing Density

4.1.1 Type of Charging Mechanism

Filter media charged by Tribo-Charging and Corona Charging were included in the study. These two charging mechanisms were included in the study to understand the effect of method of charge induction in the particle capture mechanism.

4.1.2 Type of Filtration Efficiency

In this study we have included the three filter types - N, R and P. The media used in this study is specifically used in the manufacture of dual cartridge respirator masks.

4.1.3 Packing Density

A wide range of packing densities from 50-200 g/m^2 have been looked into, to cover a large group of media.

The experimental work was divided into four tasks:

- Baseline Tests
- Identification of Chemical Degradation
- Validation of Chemical Degradation
- Storage Study

4.2 Baseline Test

The baseline study was conducted to get control data for further experiments. The results obtained from this test was used as the baseline for the future tests.

4.2.1 Experimental Setup

The baseline tests were done in accordance with the NIOSH testing protocols. The CertiTest TSI 8130 Automated Particulate Filter Tester was used for the tests. The tests were conducted at standard lab conditions of $25 \pm 5^{\circ}C$ and relative humidity of $50 \pm 5\%$. The following procedure was maintained for the baseline tests:

1. The Filter Tester was set to a challenge flow rate of 42.5 lpm.
2. The filter samples were cut into 7×7 in. squares to be placed onto 6in. wide filter holders.
3. The filter samples were weighed and placed on the filter tester.
4. Since these filters belong to a pair configuration they were loaded with 100 ± 5 mg of aerosol.
5. The loaded samples were weighed again.

Table 4.1: Filter Media Specifications

Test Code	Basis Weight (g/m^2)	Thickness (<i>mils</i>)	Fiber	Charge	NIOSH Rating for respirator masks
E1	185	39	Meltblown Polypropylene	Corona	Used in R95 DOP penetration < 0.1%@ 50lpm NaCl penetration < 0.02%@ 50lpm
E2	112	70	Meltblown Polypropylene	Corona	Used in P95 DOP penetration < 1.7%@ 50lpm NaCl penetration < 0.27%@ 50lpm
E3	150	--	Modacrylic/ Polypropylene	Tribo- Charged	DOP penetration < 50%@ 50lpm NaCl penetration < 50%@ 50lpm
E4	50	--	Meltblown Polypropylene	Corona Tantret	Used in N95 DOP penetration < 40%@ 50lpm NaCl penetration < 2.5%@ 50lpm
E5	80	--	Meltblown Polypropylene	Corona Tantret	Used in N99/R95 DOP penetration < 15%@ 50lpm NaCl penetration < 0.15%@ 50lpm
Mech	78	--	Micro-Glass Fibers	No Charge	DOP penetration < 0.075%@ 50lpm NaCl penetration < 0.02%@ 50lpm

6. The test was repeated 5 times with every filter and with both the challenge aerosols.
7. Filter Tester was calibrated daily to ensure that the aerosol distribution is optimized and has not changed.

4.3 Identification of Chemical Degradation

To evaluate the degradation mechanisms for the filter media, the filters were exposed to different chemicals that would cause a reduction in the filtration efficiency. This result would then be compared with the baseline test to comprehend the cause of the reduction and the analysis would reveal the reason for the degradation of filtration efficiency. A list of chemicals to be used was finalized after testing their reactivity with polypropylene. Various chemicals were listed and then the highly reactive chemicals were chosen from them for further research.

1. Toluene
2. HCL
3. Methyl Ethyl Ketone
4. Isopropanol
5. Water
6. Acetone
7. Hexane

4.3.1 Liquid Immersion

The filters were initially immersed in a beaker filled with the chemical for time intervals of 2, 5, 10 and 30 minutes. Later the filters were immersed in the chemicals for 2 minutes as the time interval did not have a significant influence on the filter degradation.

The following procedure was followed for the tests:

1. 3 samples of each filter media were immersed in a beaker of chemical and left for 2 minutes.
2. The filter media was then removed and dried for 24 hours.
3. After 24 hours, the filter media was the tested on the TSI 8130 Filter Tester.
4. The Filter Tester was set to challenge flow rate of 42.5lpm.
5. DOP (Di-Octyl Pthalate) was the test agent used for these tests.
6. The filters were loaded for 20 minutes, with data acquired every minute, hence 20 readings were obtained for every sample.
7. The samples were weighed before and after loading.

The chemicals that caused maximum decrease in efficiency were sorted out and then used for the vapor experiments.

4.3.2 Validation of Chemical Degradation

Once the response of the filter media to the chemicals was observed, the following set of experiments were conducted to clearly define the next step towards the research. The filter media were sprayed with Isopropanol and left to dry for 24 hours. Then these filters were exposed to vapors.

4.3.3 Chemical Exposure Apparatus

First the apparatus had to be designed to expose the filter media to chemicals. The design was fabricated by Prism Research Glass, Inc. (Research Triangle Park, NC). The glass vessel had a closed spherical bottom. A base was molded to the bottom so that the vessel would be freely standing. A groove was pressed into the edges of the glass tube that would serve, in conjunction with a fitting glass ring, as means to support the samples in the middle of the vessel. Two nozzles were attached to the

vessel on opposite sides, one above the groove and one below. The top of the vessel was enclosed with a glass lid by adding a flange and grinding the surface. The interface was sealed with inert grease. The exhaust of the exposure chamber was connected to a ventilation system and was intermittently sampled with the gas chromatograph to verify a constant solvent concentration. A schematic of the experimental setup is shown in Figure 4.1.

Nitrogen was bubbled through a three nozzle rounded vessel containing liquid solvent in order to generate a saturated vapor. Gas flow through the saturator was controlled at $1000 \text{ cm}^3\text{min}^{-1}$ using a tube flow-meter. The stream of saturated vapor was connected to the exposure chamber using Tygon tubing.

The filters were first exposed to isopropanol vapors in the chemical vapor apparatus for time interval 15, 30 minutes, 1, 2, 4, and 8 hours. Some difficulties arose as isopropanol used to condense within the pipes even before it reached the vessel.

The tests were then continued with Toluene which is a solvent commonly found in commercial environments. Toluene is commonly used in paint thinners and has a vast use in the industry as a solvent. When immersed in toluene solution, the filter media showed maximum degradation. The experiments were then continued with Xylene and Ethyl Benzene as a validation process to the experiments conducted.

Benzene, toluene, ethylbenzene, and xylene frequently occur together at hazardous waste sites. These four chemicals are volatile and have good solvent properties. Toxicokinetic studies in humans and animals indicate that these chemicals are well absorbed, distribute to lipid-rich and highly vascular tissues such as the brain, bone marrow, and body fat due to their lipophilicity, and are rapidly eliminated from the body. The mixture of these solvents is generally termed as BTEX (Benzene, Toluene, Ethyl Benzene, Xylene). All four chemicals can produce neurological impairment via parent compound-induced physical and chemical changes in nervous system membranes.

Hence the three chemicals - Toluene, Xylene and Ethyl Benzene - form an interesting study to understand the interaction of chemical and filter media used in respiratory masks.

Following experimental procedure was followed for the Vapor experiments:

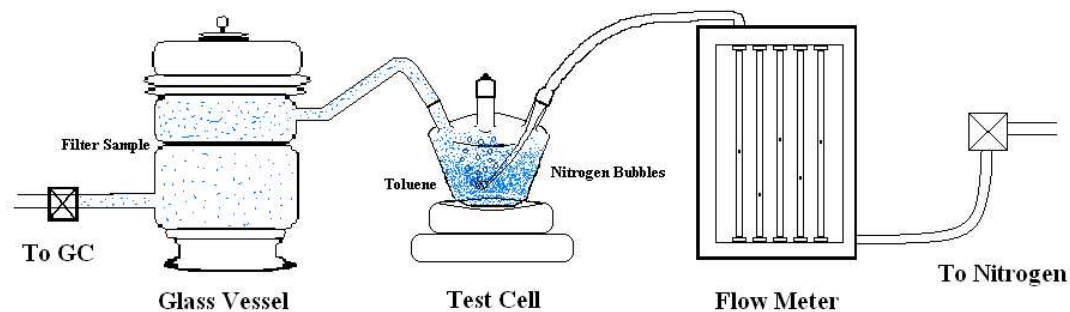


Figure 4.1: Experimental Setup for Chemical vapor exposure tests

1. 3 samples of each filter were exposed to the chemicals in a closed environment.
2. The vapor was allowed to flow at saturation.
3. Nitrogen was bubbled through the chemical at 1lpm.
4. The exposed filters were then tested on the TSI 8130 for 20 minutes.

Four different types of flow were tried out:

1. The first set of experimental conditions introduced the saturated gas into the exposure apparatus using the upper nozzle and exhausting through the lower one. This set of experimental conditions will be labeled as *downward flow*.
2. The second set of experimental conditions introduced the saturated gas into the exposure chamber through the lower nozzle, and will be referred to as *upward flow*.
3. The third experimental condition resembles Condition 1 as the flow inside the chamber is downward with the difference that dry-ice packs were placed at the outside lower nozzle in order to generate condensation of toluene and hence a two-phase flow.
4. The fourth experimental condition introduced the saturated gas into the exposure chamber using the lower nozzle and exhausts through the upper nozzle like

condition 2, except that dry-ice packs were placed in the lower nozzle. This condition is referred to as *ice-bath upward flow*.

During experimental Conditions 3 and 4 (ice-bath downward and ice-bath upward flow), liquid chemical was observed at the bottom of the exposure chamber confirming the presence of a two-phase flow. It was evident that only during experimental Condition 3 (ice-bath downward flow) was the filter media directly exposed to the liquid chemical. In order to determine the flux of chemical liquid and gas through the exposure chamber, thermodynamic simulations were performed.

Chapter 5

Results and Discussion

5.1 Baseline Tests

The baseline tests were conducted to obtain standard data for the filtration behavior of these non-woven media. As mentioned in the previous chapter the tests were conducted according to the procedure mentioned in 42 CFR Part 84.

5.1.1 R and P Rated Filters

The R and P rated filters are corona charged filter media. The R and P ratings stand for oil resistance and oil proof finish respectively, which enables the filter media to perform efficiently against the liquid aerosols. The curve shown below demonstrates the filter media being loaded with DOP. The media was loaded up to 100mg of aerosol. The percent penetration data was plotted against time of loading. Data was captured every minute. Both percent penetration of filter media and the pressure drop across the filter media has been plotted against time. The graph shows the filtration behavior of the filters with respect to time.

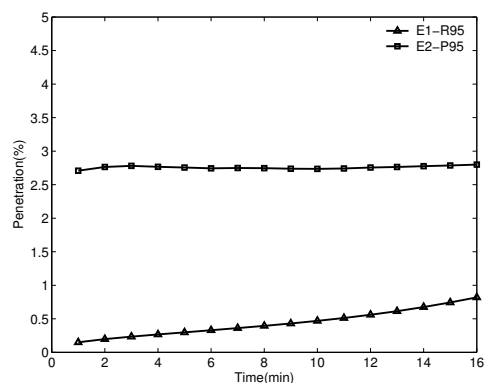


Figure 5.1: Penetration Curve for the filter loaded with DOP

Both the graphs show the filtration curve for the corona charged R and P rated filters. The filters give an efficiency more than 95% filtration. It is usually observed that DOP degrades the charge on the fiber surface when exposed for prolonged durations. These filters have open structure and hence lower resistance.

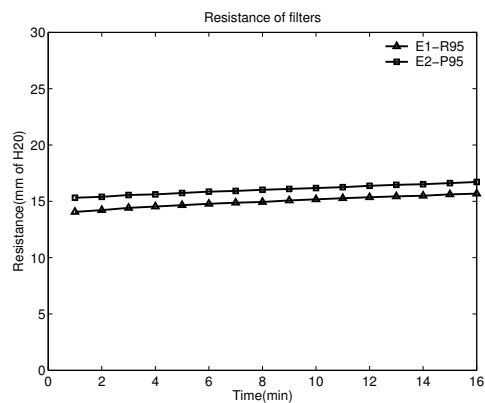


Figure 5.2: Resistance Curve for the filter loaded with DOP

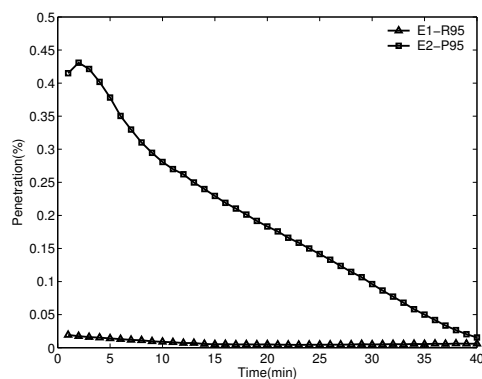


Figure 5.3: Penetration Curve for the filter loaded with NaCl

As seen in the literature review of the mechanism of filtration for solid particles, the experimental work done shows the mechanism involved. The filtration efficiency of the filter decreases initially as the filters gets caked because of screening of charges. Then the efficiency increases as caking occurs and the filter starts behaving like a mechanical filter.

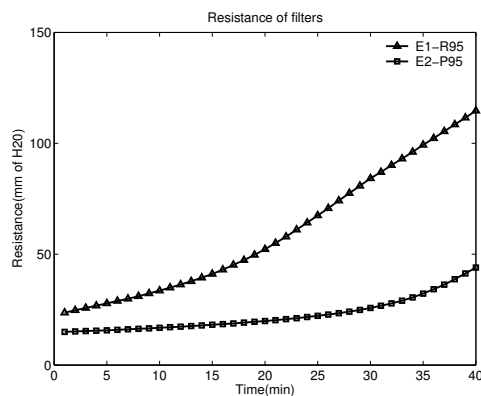


Figure 5.4: Resistance Curve for the filter loaded with NaCl

5.1.2 N Rated Filters

The N rated filters are not used for liquid aerosols. They are known as the non oil filters, used only for protection against solid particles.

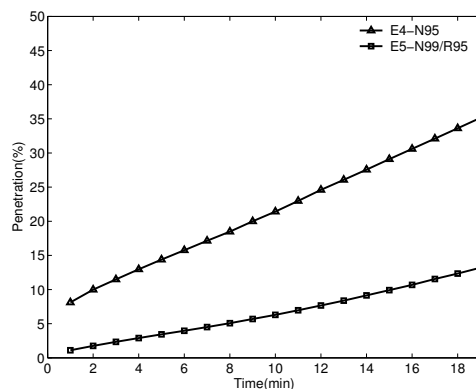


Figure 5.5: Penetration Curve for the filter loaded with DOP

As seen from the graph, the filter media does not perform well when exposed to DOP. A higher penetration is observed for E4, a N-95 filter. The filter media also has the least basis weight. As mentioned in the filter specifications, the filter media is used in masks as layers. The resistance for these filter media is also lower than the other filters.

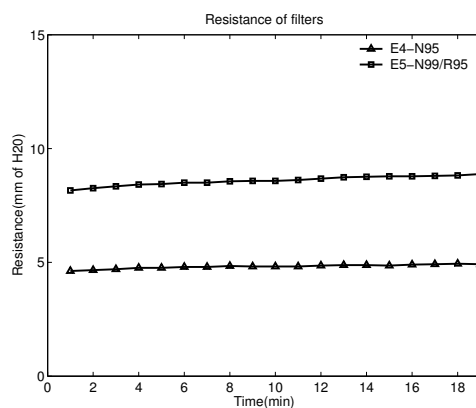


Figure 5.6: Resistance Curve for the filter loaded with NaCl

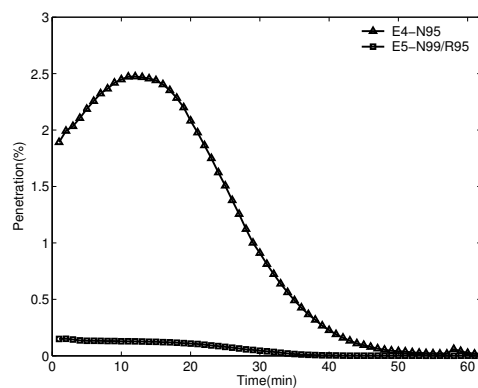


Figure 5.7: Penetration Curve for the filter loaded with NaCl

The Figure here show an initial rise in the penetration and then a steep decline. As seen from the figure, the *N99/R95* filter shows a better response to NaCl particles but does not work too well with DOP aerosol.

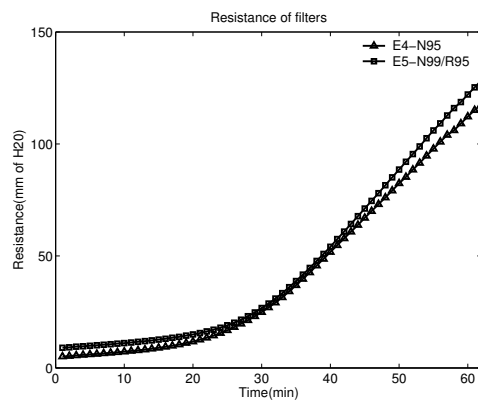


Figure 5.8: Resistance Curve for the filter loaded with NaCl

5.1.3 Tribo Charged Filters

The tribo charged filters are needle punched filter media with two different fiber types, mixed together to create a field on the surface due to tribo electric exchange.

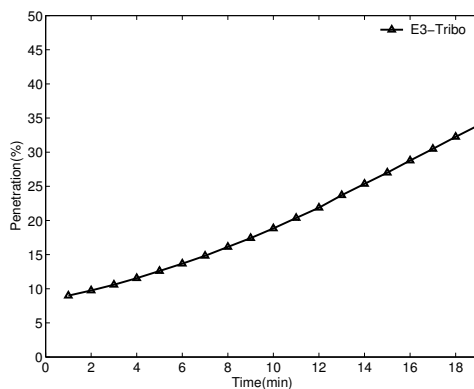


Figure 5.9: Penetration Curve for the filter loaded with DOP

These filters show high penetration with extremely low resistance.

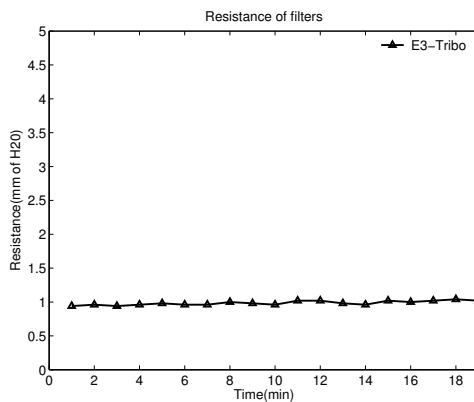


Figure 5.10: Resistance Curve for the filter loaded with DOP

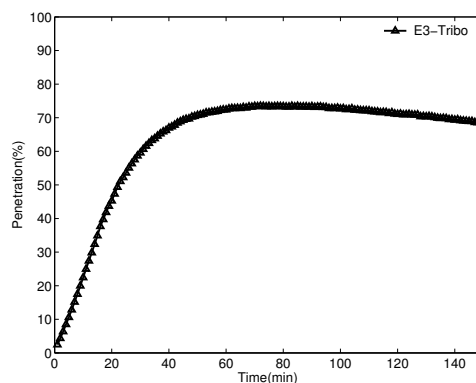


Figure 5.11: Penetration Curve for the filter loaded with NaCl

A higher penetration is demonstrated by these filters for NaCl particles. The ionic particles tend to reduce the efficiency more than the liquid particles. The open structure does not tend to clog as quickly as mechanical filter, as seen from the slight increase in the resistance data.

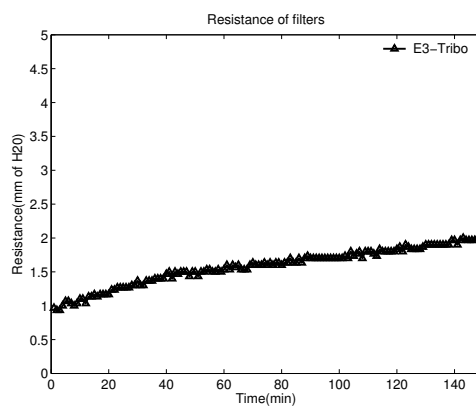


Figure 5.12: Resistance Curve for the filter loaded with NaCl

5.1.4 Mechanical Filter

The mechanical filters do not have any charge on the filter surface. Hence the filter is more compact, stiff and has a higher packing density to capture the micro-sized aerosols.

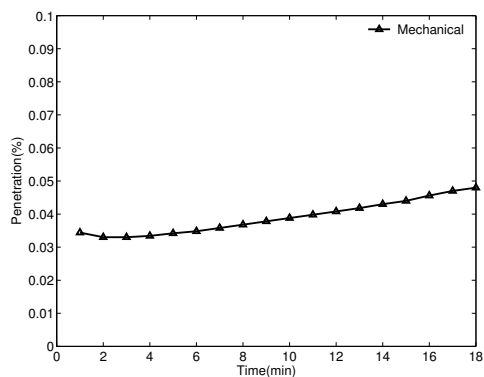


Figure 5.13: Penetration Curve for the filter loaded with DOP

These filters display the least penetration percentage, but with the highest resistance. The resistance values are twice when compared to the electret filter media.

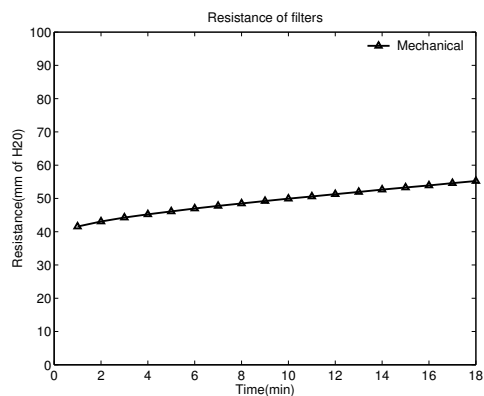


Figure 5.14: Resistance Curve for the filter loaded with DOP

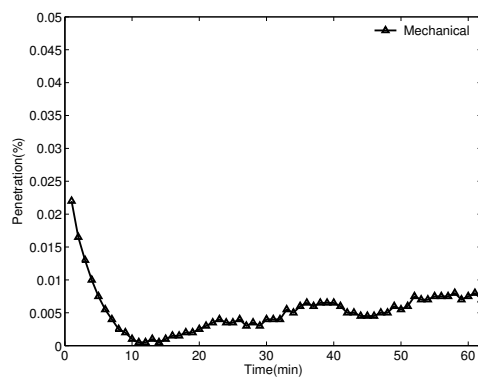


Figure 5.15: Penetration Curve for the filter loaded with NaCl

The filter media shows 99% efficiency but with 3 times the pressure drop.

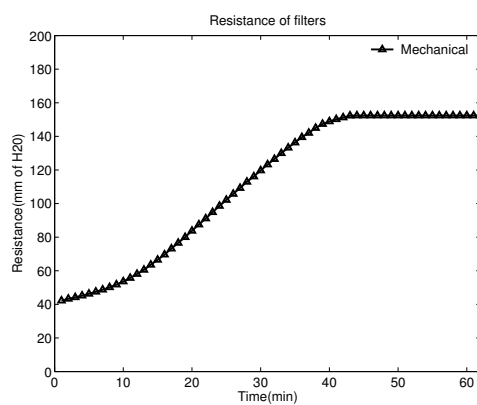


Figure 5.16: Resistance Curve for the filter loaded with NaCl

Summary

On analyzing the graphs, we observe a higher filtration efficiency for solid particles. While the pressure drop remains steady for the liquid particles, the pressure drop for the filter media loaded with solid salt aerosols undergoes a steep rise in value. The point where the slope takes a sudden vertical bend is termed as the clogging point. As has been discussed in literature review, it is the point from where on the electret filter media starts behaving like a mechanical filter. Hence both the aerosols show a degrading effect on the filter media. The liquid particles coat the fibers, hence reducing the filtration efficiency and masking the electrostatic charge on the filter media. This phenomenon can be validated as the liquid aerosols do not affect the physical properties of the filter media as no change in the resistance is observed. The solid particles on the other hand, clog the interstices causing an increase in the filter resistance. Caking on the surface most probably screens out the electrostatic charge on the filter media.

The different media types show varied filtration efficiency. The R and P rated filters show higher efficiencies for both DOP and NaCl particles as they are oil proof and oil resistant. While the N rated filters perform poorly for DOP aerosols.

The basis weight of the filters also has an influence on the filtration. The R and P rated filters have higher basis weight, hence show good efficiency but with higher resistance. The N rated filters show slightly higher penetration of aerosols but with lower resistance. It has also been specified by the manufacturers that these filter media are to be used in layers.

5.2 Investigation of Chemical Degradation

The first experimental set was to immerse these filters in the liquid solvents and later to expose them to vapors and observe the effect the solvents had on the filtration. The filters were dipped in beakers filled with chemicals, for 2 minutes and later allowed to dry for 24 hours.

5.2.1 Liquid Immersion

Filters Immersed in Water

E1-R95:Corona Charged Filter

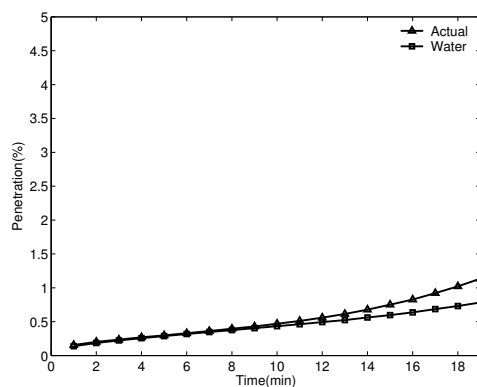


Figure 5.17: Penetration Curve for the filter immersed in Water

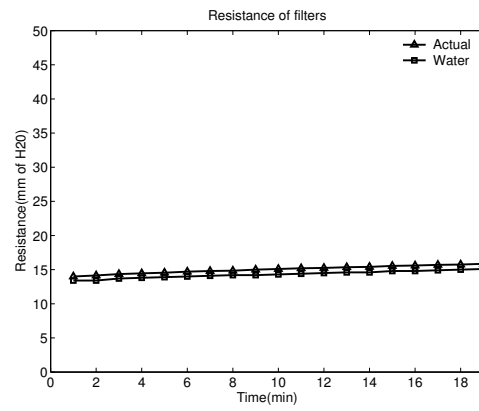


Figure 5.18: Resistance Curve for the filter immersed in Water

E2-P95 Corona Charged Filter

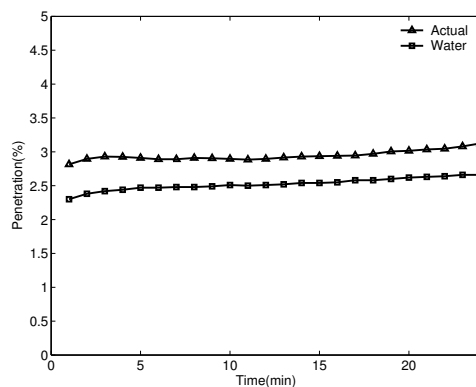


Figure 5.19: Penetration Curve for the filter immersed in Water

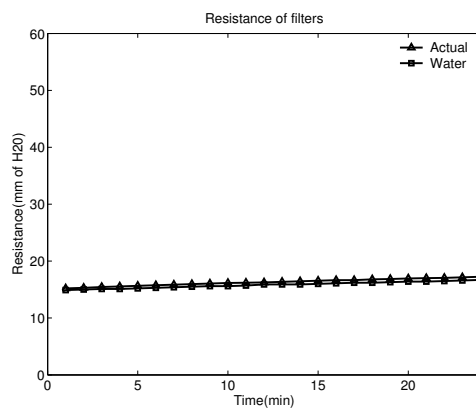


Figure 5.20: Resistance Curve for the filter immersed in Water

E5-N99/R95 Tantret Corona Charged Filter

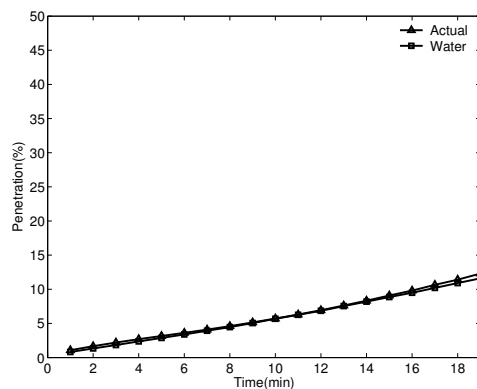


Figure 5.21: Penetration Curve for the filter immersed in Water

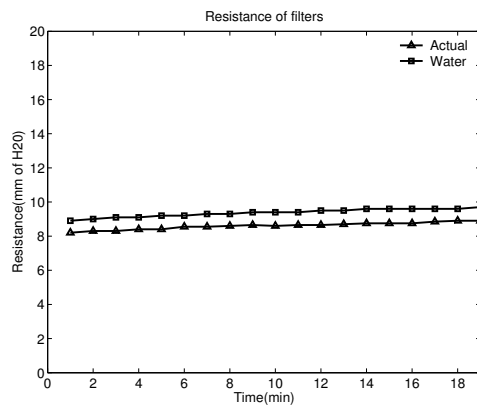


Figure 5.22: Resistance Curve for the filter immersed in Water

Mechanical Filter- Microglass Fibers

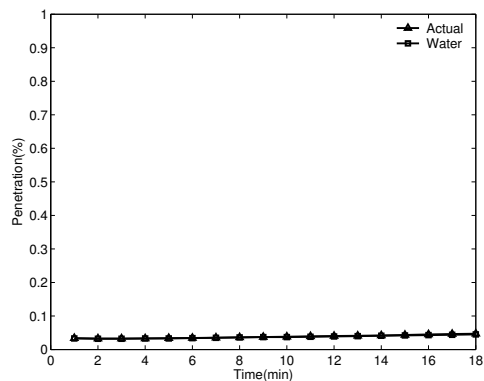


Figure 5.23: Penetration Curve for the filter immersed in Water

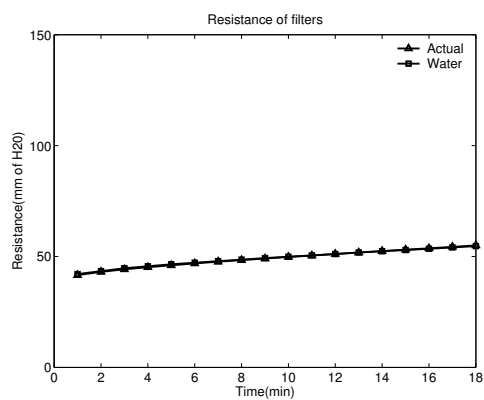


Figure 5.24: Resistance Curve for the filter immersed in Water

Summary

Even though water has high polarity, it does not seem to effect the filtration mechanism in the filter media. This could be related to the fact that both polypropylene and glass are hydrophobic. There was no physical swelling observed when the filters were immersed in water. After removal, the beaded water droplets were observed on the filter surface.

Filters Immersed in Acetone

E1-R95 Corona Charged Filter

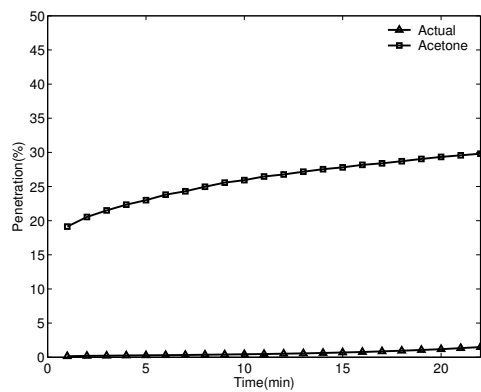


Figure 5.25: Penetration Curve for the filter immersed in Acetone

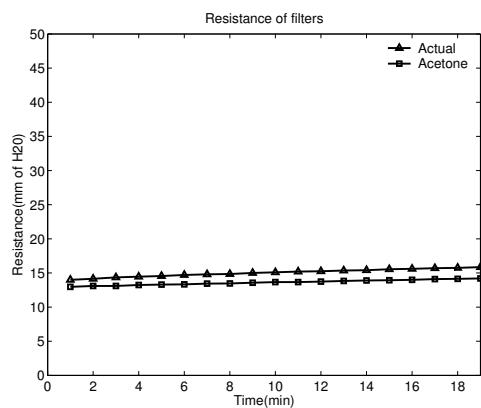


Figure 5.26: Resistance Curve for the filter immersed in Acetone

E2-P95 Corona Charged Filter

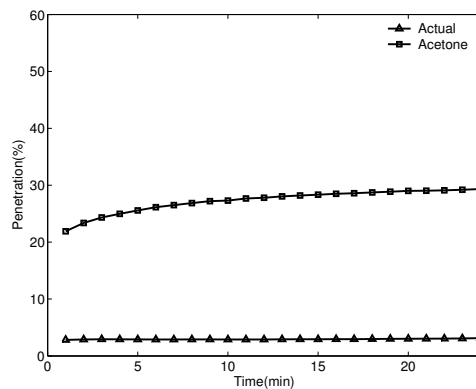


Figure 5.27: Penetration Curve for the filter immersed in Acetone

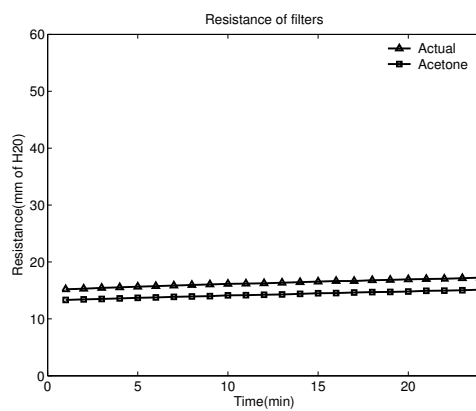


Figure 5.28: Resistance Curve for the filter immersed in Acetone

E5-N99/R95 Corona Charged Filter

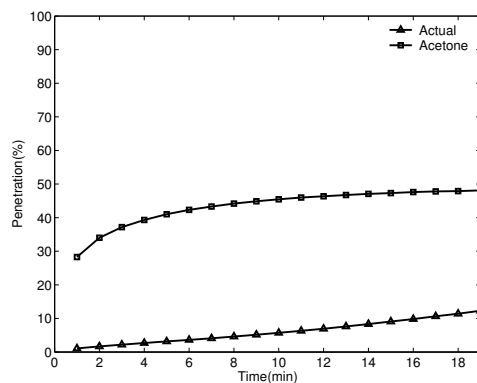


Figure 5.29: Penetration Curve for the filter immersed in Acetone

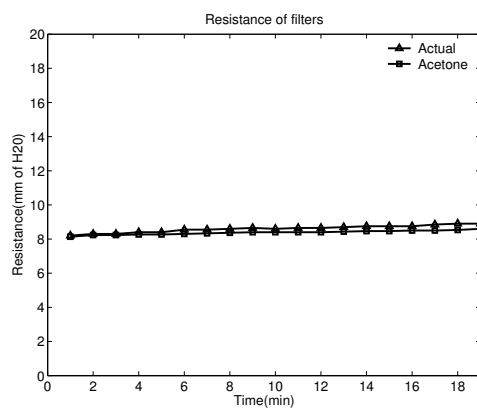


Figure 5.30: Resistance Curve for the filter immersed in Acetone

Mechanical Filter-Microglass Fiber

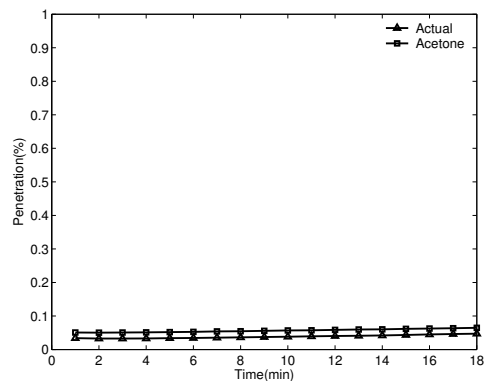


Figure 5.31: Penetration Curve for the filter immersed in Acetone

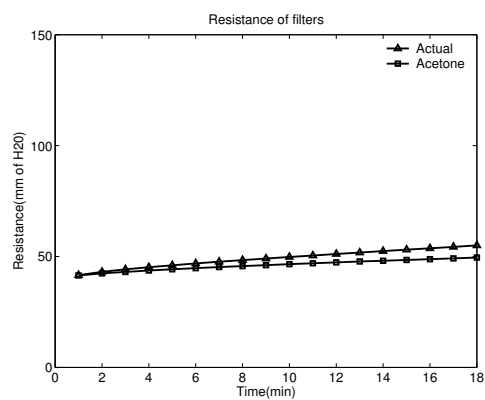


Figure 5.32: Resistance Curve for the filter immersed in Acetone

Summary

The electret filters seem to show a significant amount of degradation with acetone. Polypropylene dissolves in acetone, while the mechanical filter was not affected by the solvent. Acetone is quite a common solvent used in industry. Hence a direct exposure to liquid acetone will have a degrading and dangerous effect on these filter media as they will lose their efficiency. Hence the filter media will not be of any use or protection from particles in the most penetrating particle size. Another important point to note is that the filters do not show any significant change in the pressure drop. Hence it can be concluded that the chemical does not seem to have any effect on the physical state of the filter media. Further on it shall be shown how the other chemicals also have a similar reaction to the filter media.

Filters Immersed in Methyl Ethyl Ketone

E1-R95 Corona Charged Filter

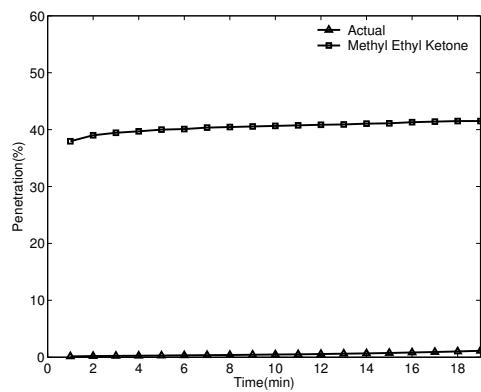


Figure 5.33: Penetration Curve for the filter immersed in Methyl Ethyl Ketone

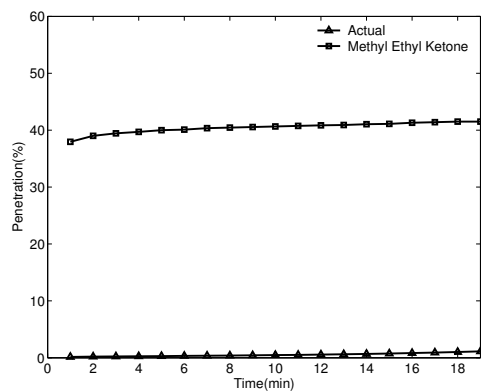


Figure 5.34: Resistance Curve for the filter immersed in Methyl Ethyl Ketone

E2-P95 Corona Charged Filter

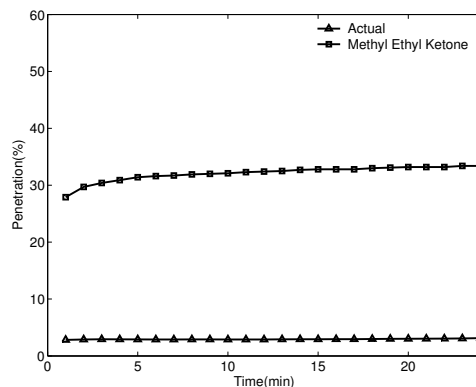


Figure 5.35: Penetration Curve for the filter immersed in Methyl Ethyl Ketone

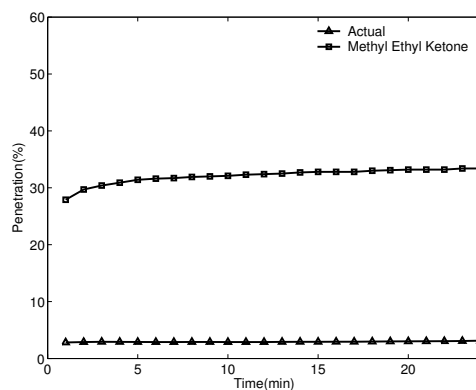


Figure 5.36: Resistance Curve for the filter immersed in Methyl Ethyl Ketone

E5-N99/R95 Tantret/Corona Charged Filter

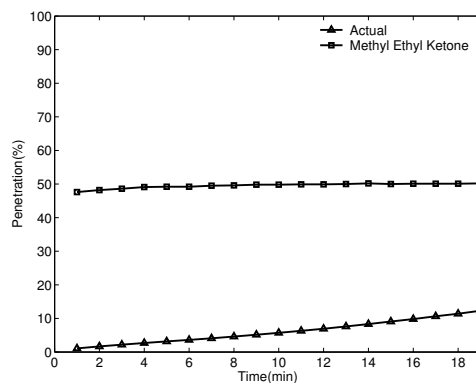


Figure 5.37: Penetration Curve for the filter immersed in Methyl Ethyl Ketone

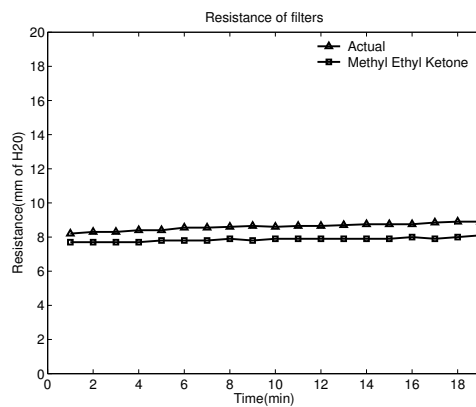


Figure 5.38: Resistance Curve for the filter immersed in Methyl Ethyl Ketone

Mechanical Filter-Microglass Fiber

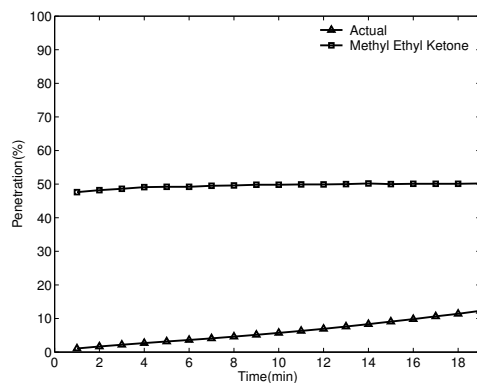


Figure 5.39: Resistance Curve for the filter immersed in Methyl Ethyl Ketone

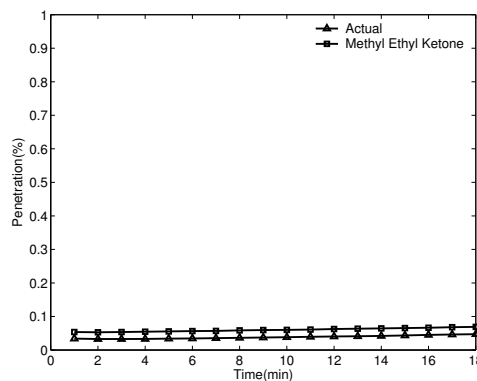


Figure 5.40: Resistance Curve for the filter immersed in Methyl Ethyl Ketone

Filters Immersed in Hexane

E1-R95 Corona Charged Filter

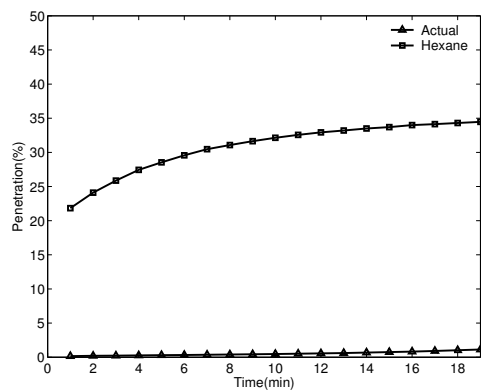


Figure 5.41: Penetration Curve for the filter immersed in Hexane

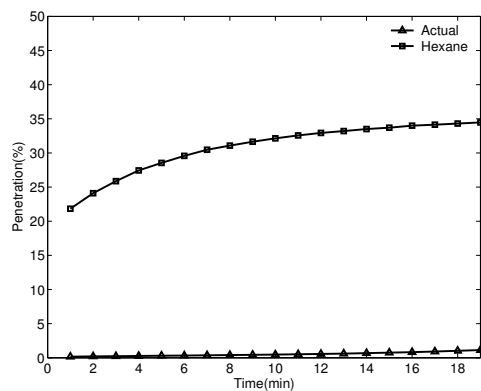


Figure 5.42: Resistance Curve for the filter immersed in Hexane

E2-P95 Corona Charged Filter

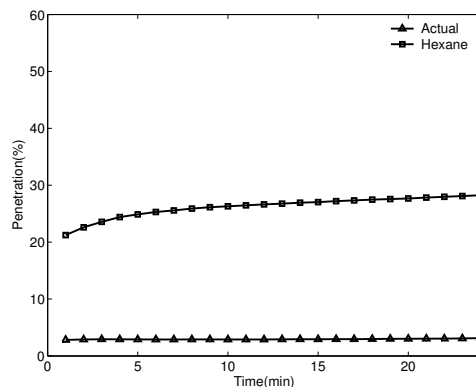


Figure 5.43: Penetration Curve for the filter immersed in Hexane

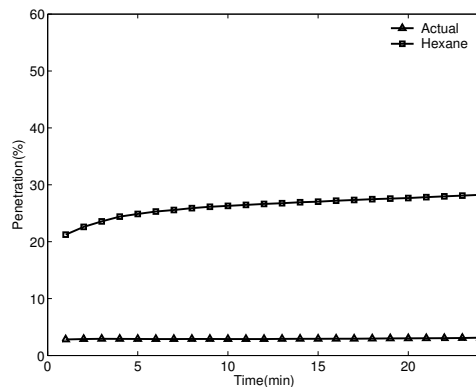


Figure 5.44: Resistance Curve for the filter immersed in Hexane

E5-N99/R95 Tantret/Corona Charged Filter

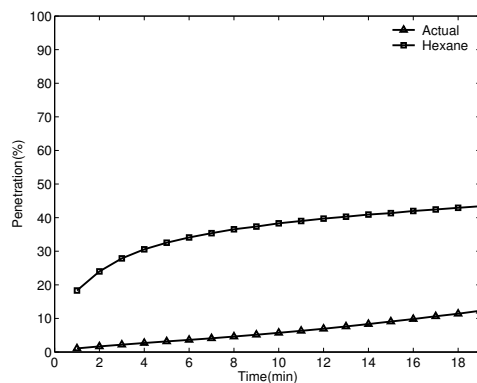


Figure 5.45: Penetration Curve for the filter immersed in Hexane

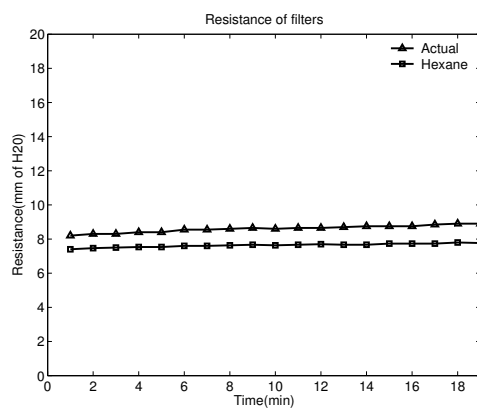


Figure 5.46: Resistance Curve for the filter immersed in Acetone

Mechanical Filter-Microglass Fiber

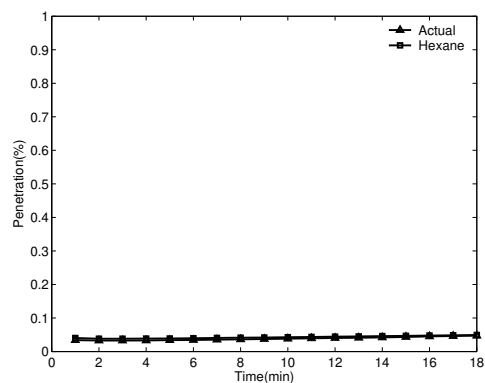


Figure 5.47: Resistance Curve for the filter immersed in Hexane

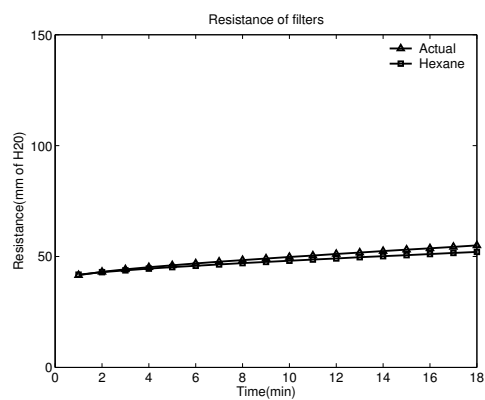


Figure 5.48: Resistance Curve for the filter immersed in Hexane

Filters Immersed in Toluene

E1-R95 Corona Charged Filter

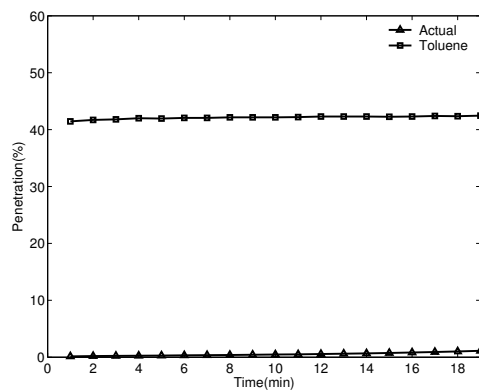


Figure 5.49: Penetration Curve for the filter immersed in Toluene

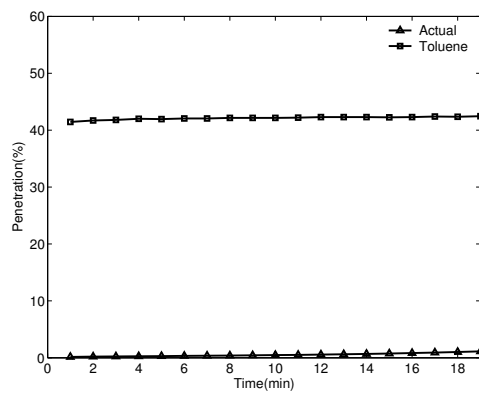


Figure 5.50: Resistance Curve for the filter immersed in Toluene

E2-P95 Corona Charged Filter

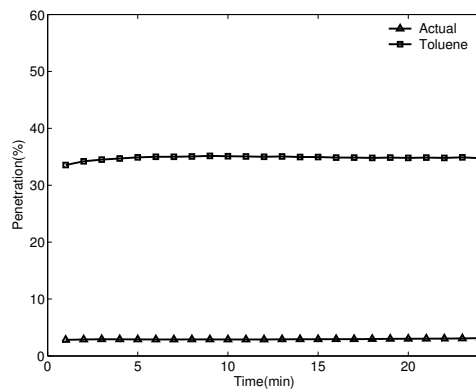


Figure 5.51: Penetration Curve for the filter immersed in Toluene

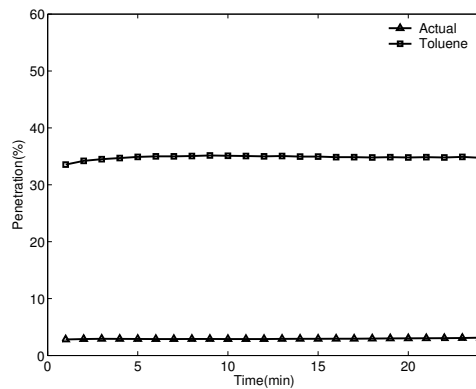


Figure 5.52: Resistance Curve for the filter immersed in Toluene

E5-N99/R95 Tantret/Corona Charged Filter

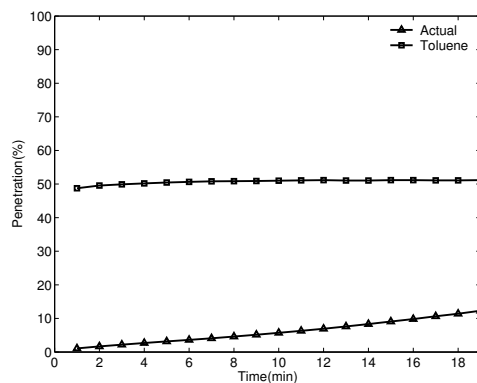


Figure 5.53: Penetration Curve for the filter immersed in Toluene

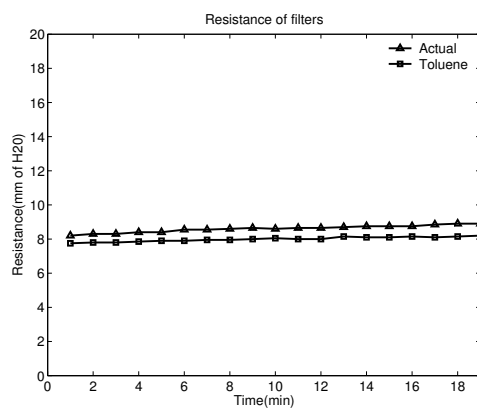


Figure 5.54: Resistance Curve for the filter immersed in Toluene

Mechanical Filter-Microglass Fiber

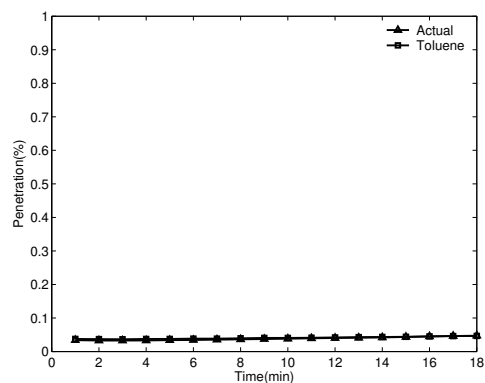


Figure 5.55: Resistance Curve for the filter immersed in Toluene

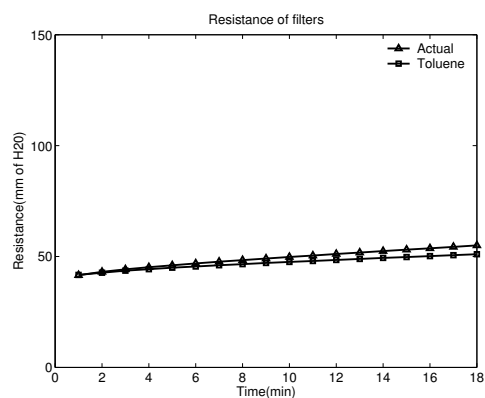


Figure 5.56: Resistance Curve for the filter immersed in Toluene

Summary

The solvents seem to show a high degrading effect on the filtration efficiency. They seem to dissipate the charge off, as the electret media seems to work like a mechanical filter. Toluene seems to show quite high an effect on the filtration efficiency, though none of the solvents seem to have any significant effect on the pressure drop.

5.2.2 Vapor Exposure

After analyzing the results obtained from the liquid immersion tests, the filter media were exposed to the solvent vapors at saturation. Toluene was chosen as it had the highest impact on filtration. Also Toluene also has a wide application in the industry, hence makes a useful tool for the study.

The first tests done were with downward flow. The solvent was passed through the filter media for different intervals of time. But no significant degradation was observed.

Later the experiments were modified and four different types of flows were analyzed. The different flows have been clearly explained in the Research Approach.

The experimental work was then narrowed down to the hazardous chemicals termed as BTEX (Benzene, Toluene, Ethyl Benzene and Xylene). Three of the solvents in this group were used to obtain a strong validation for the tests performed and also to reduce the amount of variation in the setup.

5.2.3 Toluene Exposure

E1-R95 Corona Charged Filter

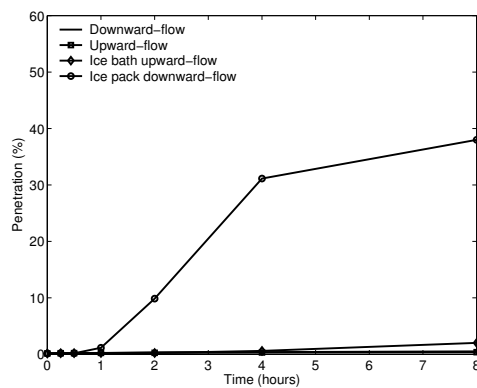


Figure 5.57: Penetration Curve for the filter exposed to Toluene

E2-P95 Corona Charged Filter

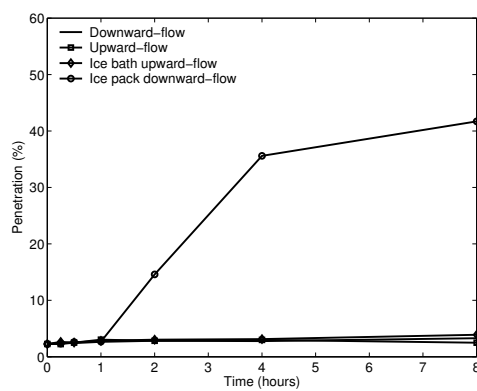


Figure 5.58: Penetration Curve for the filter exposed to Toluene

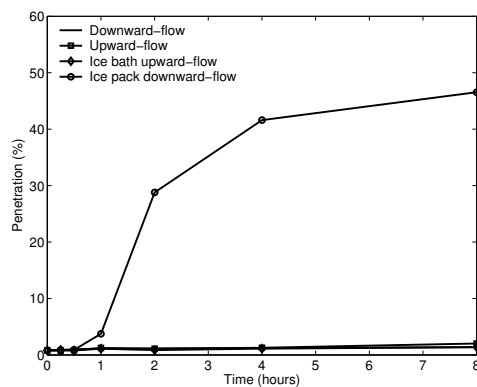
E5-N99/R95 Tantret/Corona Charged Filter

Figure 5.59: Penetration Curve for the filter exposed to Toluene

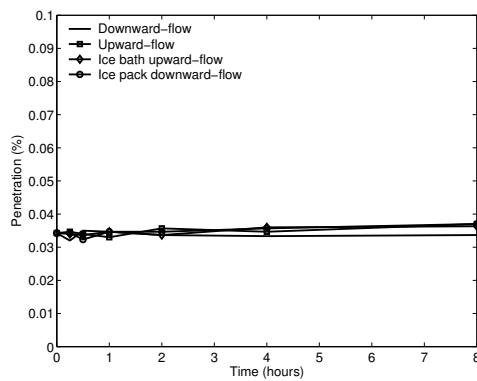
Mechanical Filter-Microglass Fiber

Figure 5.60: Penetration Curve for the filter exposed to Toluene

5.2.4 Xylene Exposure

E1-R95 Corona Charged Filter

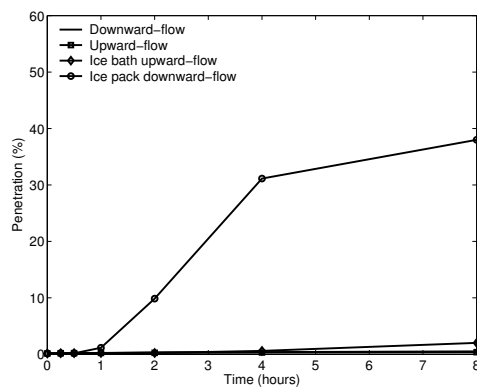


Figure 5.61: Penetration Curve for the filter exposed to Xylene

E2-P95 Corona Charged Filter

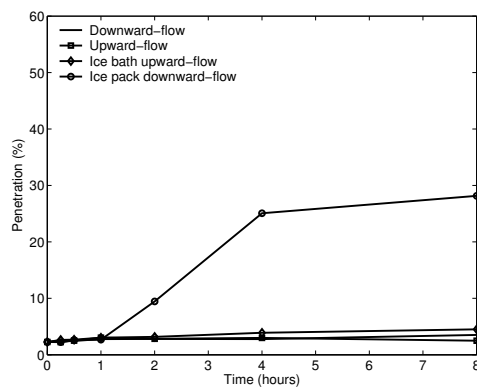


Figure 5.62: Penetration Curve for the filter exposed to Xylene

E5-N99/R95 Tantret/Corona Charged Filter

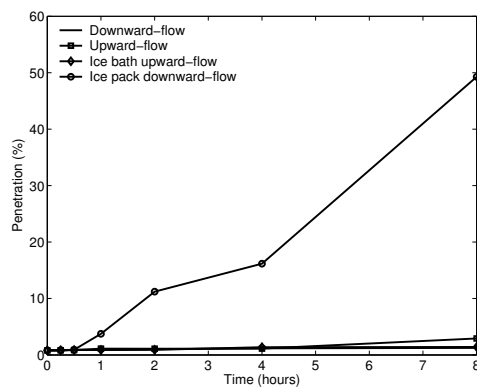


Figure 5.63: Penetration Curve for the filter exposed to Xylene

Mechanical Filter-Microglass Fiber

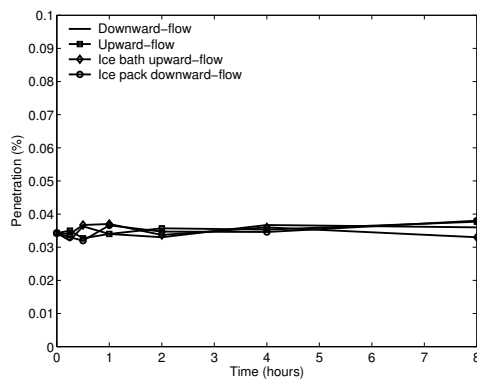


Figure 5.64: Penetration Curve for the filter exposed to Xylene

5.2.5 Ethyl Benzene Exposure

E1-R95 Corona Charged Filter

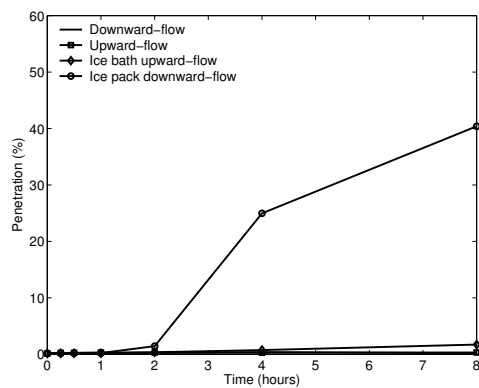


Figure 5.65: Penetration Curve for the filter exposed to Ethyl Benzene

E2-P95 Corona Charged Filter

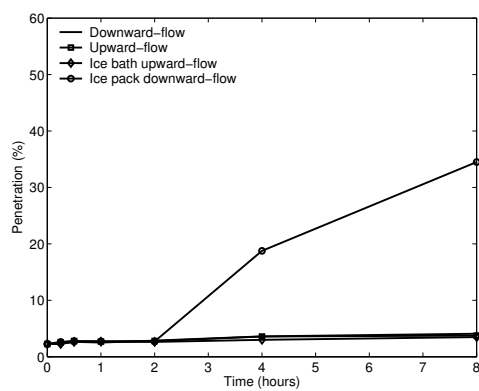


Figure 5.66: Penetration Curve for the filter exposed to Ethyl Benzene

E5-N99/R95 Tantret/Corona Charged Filter

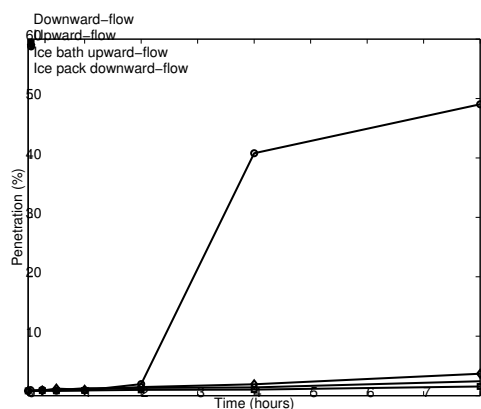


Figure 5.67: Penetration Curve for the filter exposed to Ethyl Benzene

Mechanical Filter-Microglass Fiber

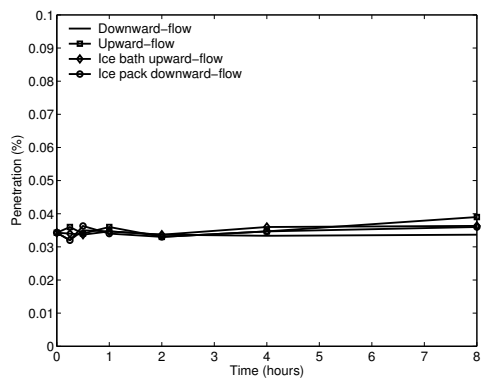


Figure 5.68: Penetration Curve for the filter exposed to Ethyl Benzene

Summary

The filters show a significant amount of degradation when exposed to condensed solvent. In the Icepack Downward Flow, the solvent got condensed due to the cold and fell onto the filter media hence degrading the filter media. While the rest of the flows do not seem to show any significant change in the filter media.

It could be inferred from this experimental work that these solvents cause charge dissipation in the filter, in liquid phase.

Chapter 6

Conclusion

This study gives a comprehensive, while quite conclusive data on the effect of chemicals on the filter media.

The work clearly shows how the filter media is affected by liquid solvents. While different chemicals seem to show slight variation in the effect, a general idea can be framed from the results that the chemicals that are reactive to polypropylene show reduction in the filtration efficiency in liquid phase.

Also these results validate the ones shown by other authors that chemicals in vapor form do not affect the filtration efficiency of the filter media. The filters have strong charge retention, hence vapors or the atmospheric conditions do not seem to show any significant effect on the filter media. The vapors at saturation simulate the extreme case of exposure. Hence it could be safely said that these filter media can sustain a extreme exposure of hazardous vapors and still filter out particles.

A general study of the manufacturing technique shows that the bonds in the fibers are relaxed due to heat while the charges are bombarded onto the fiber surface. Hence the bonds get oriented and this orientation holds the charge in the form of a dipole in the fiber.

We can hypothesize that the chemical absorbed by the fiber causes it to relax and the bonds loosen up which causes the dipole moments to reorient. This might result in the dissipation of the charge from the fiber. All the chemicals were dried out before the efficiency was tested hence no significant change was observed in the resistance of these media to the aerosols. The chemicals could have caused some swelling that

might have dissipated the charge from the filter media.

Chapter 7

Appendix

7.1 Instrument Setup and Usage

The filter media were tested on a TSI 8130 CertiTest Automated Filter Testers. The tester uses two laser-based light scattering photometers to measure the concentration of fine aerosol particles upstream and downstream of the filter or filter media under test. The particles are produced by an oil or salt aerosol generator incorporated in the filter tester. Laser light, focused on the particle stream, is scattered by the aerosol particles. The scattered light is collected by a photo detector, producing a signal level proportional to particle concentration. Filter penetration is determined from the ratio of the particle concentrations measured before and after the filter.

7.2 Aerosol Generation

The Model 8130 incorporates a unique oil and salt aerosol generators developed by TSI specifically for filter testing applications. The TSI generators use atomizer jets to disperse a liquid oil or salt solution into small droplets. These droplets form an aerosol which is then passed through a special felt coalescing filter for oil or an impactor for salt. The process produces an aerosol with a size distribution that closely matches that of an ideal test aerosol, one which has a mean centered in the range of (MMPS) 'most penetrating size range'.

The oil generator uses a narrow size distribution without using heat to condition

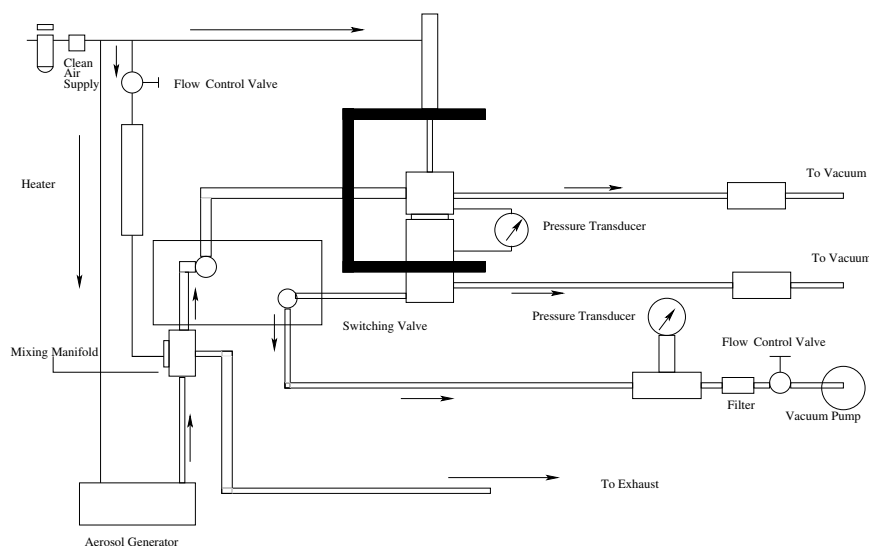


Figure 7.1: Schematic Diagram of Automated Filter Tester

the aerosol. No heat means a variety of oils can be associated with the use of di-octyl phthalate (DOP).

7.3 Aerosol Mixing and Transport

A main component in the instrument is the aerosol transport system. Aerosol particles produced by the aerosol generators are drawn into and through a mixing manifold, through the upstream filter holder and photometer, through the filter under test, and through the downstream filter holder and photometer using a vacuum pump.

In the mixing manifold, aerosol is mixed with clean make-up air supplied at a constant rate. The upstream aerosol concentration is thereby maintained constant and independent of the filter flow rate.

The filter testers are configured so that the aerosol flows from top to bottom.

7.4 Particle Detectors

The Automated Filter Testers employ light scattering photometer technology for aerosol detection. Photometers, unlike single particle counting instruments, rely on light scattering from multiple particles to obtain a relative concentration measurement. If the aerosol composition is controlled, as in a TSI filter tester, photometer signal output is linear with particle concentration.

The tester uses two stable, solid-state, laser-based photometers calibrated against one another. One is dedicated to measuring the particle concentration upstream of the filter being tested, the other to measuring the downstream concentration. A representative particle sample is drawn from the particle stream, combined with a filtered sheath air stream, and directed through the photometer. The sheath air serves to define the particle stream, improving the photometer performance, and keep the internal optics clean.

The upstream photometer is a simple device offering relatively low resolution, since it only needs to measure the high upstream particle concentration. The downstream photometer, on the other hand, uses a high power laser diode and offers much higher resolution in order to measure the very low downstream concentrations necessary when making penetration measurements down to 0.001 point.

Concentration is determined from the photometer output signal voltage. The signal voltage is proportional to the mass of aerosol sampled by the photometer. When calculations are performed by the tester firmware, the background voltage is subtracted from the total signal voltage. The background voltage is produced by the photometer when no aerosol is present.

7.5 Microprocessor Control

The CertiTest Filter testers are controlled by a microprocessor and user-friendly software resident in a 64k EPROM. The microprocessor provides automatic control of all tester operations, based on parameters specified by the operator and inputs from the photometers, pressure transducer, touch-display panel and filter holder close buttons.

The microprocessor calculates information on the filter penetration and resistance over a wide range of filter flow conditions. It also performs operational self checks during testing to ensure test accuracy. System status information and operator instructions are presented on an easy to read touch panel display.

The microprocessor and the built-in software greatly simplify system operation, reducing the training required to run the system effectively. Simple software menus allow the operator to change tests parameters to accommodate special testing or research requirements. An RS-232 serial interface provides a means for outputting test data to an external computer or data logging device. A special, built in interface also provides the capability for external tester control. This feature facilitates filter testing using automated (robotic) filter insertion and removal.

7.6 Data Acquisition System

A system for collecting data from the filter test experiments has been developed and is now being utilized. The system consists of the 8130 system itself, a data collection computer, and a new database application. In the system, a data collection computer is connected to the 8130 filter tester using the standard RS-232 communication port available on the 8130. Data is captured by the computer using Hyper Terminal, a standard communications tool in the MS Windows® suite of tools. The data is then loaded to a database and stored. A diagram of the database is shown in Figure 7.2.

The database has four interrelated areas for storing information about each filter test. The first is the TestSample area where general information about the test is stored. Examples would be challenge agent, filter type, test agent, exposure time, etc. The second area contains specific information about the challenge agent that the filter was exposed to. The third area is storage for the test results and the fourth area is for storing specific data about the filter itself. Examples would be the filter manufacturer, the fiber type, and the charging process. A software tool called MySQL has been selected for construction of the database because of its ease of operation and its compatibility with both Windows and Linux operating systems. Java is being used to generate input/output applications for the database because of

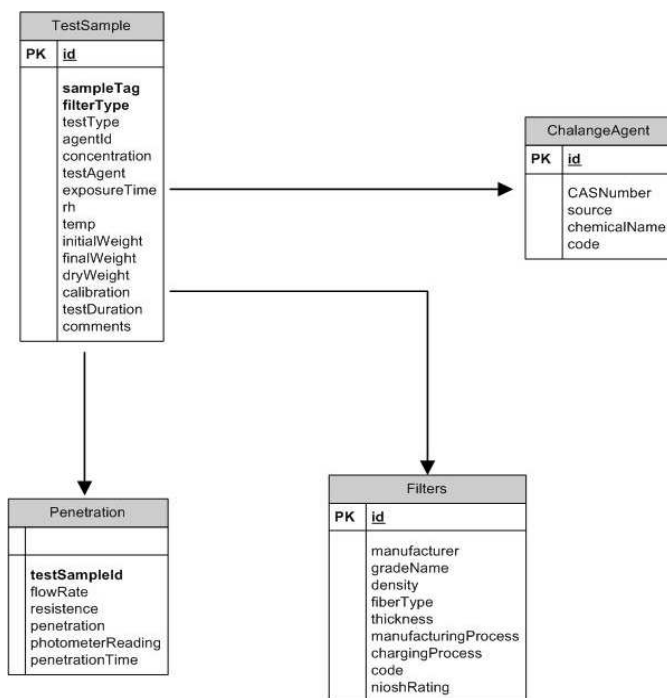


Figure 7.2: Block Diagram-Data Collection Database

its platform independence. The application has been optimized for storage size and speed by choosing relational entity scheme. An example of an input/output window is shown in Figure 7.3 .

The application is capable of:

Allowing users to enter test sample generic data and save it into database. It accepts the penetration data into a table and attaches it with the test sample generic data. The data acquisition software also provides search capability. The test results are reviewed at the analyze tab to study various statistical information for each test. The mean, the standard deviation, the variance, the maximum and the minimum values of penetration of each test sample can easily be viewed. Upon selecting a particular test, the details of the test along with the penetration values can be accessed by switching to the 'Data Entry' tab. The latest version of the software now also supports deletion of the viewed sample to eliminate any wrong data inserted into the database.

The screenshot shows the NCSU CertTester application window. On the left is a 'Data Entry' form with fields for Sample Tag, Test Type (2LYR), Chemical Agent, Concentration (%), Test Agent (DOP), Chemical Exposure Time (min), Room RH (%), Temperature (Celsius), Dry Weight (grams), Initial Weight (grams) (7.357), Final Weight (grams) (7.461), Filter (E3), Calibration?, Test Duration (min) (24), Penetration File Path, and Comments. On the right is a table with columns: Flow Rate(l/min), Resistance(mm of ...), Penetration(%), Photometer Readin., and Timestamp. The table contains 20 rows of data.

Flow Rate(l/min)	Resistance(mm of ...)	Penetration(%)	Photometer Readin.	Timestamp
42.5	1.7	9.97	117.41	03.03.0004-10.53
42.5	1.7	9.23	119.81	03.03.0004-10.52
42.5	1.7	8.57	118.76	03.03.0004-10.51
42.5	1.7	7.94	114.5	03.03.0004-10.50
42.6	1.6	7.34	113.95	03.03.0004-10.49
42.5	1.7	6.74	116.86	03.03.0004-10.48
42.5	1.7	6.17	117.16	03.03.0004-10.47
42.6	1.6	5.67	114.14	03.03.0004-10.46
42.6	1.6	5.24	113.08	03.03.0004-10.45
42.5	1.7	4.74	116.86	03.03.0004-10.44
42.5	1.7	4.31	113.16	03.03.0004-10.43
42.5	1.6	3.94	113.77	03.03.0004-10.42
42.5	1.6	3.57	111.87	03.03.0004-10.41
42.5	1.6	3.25	110.65	03.03.0004-10.40
42.5	1.6	2.93	110.03	03.03.0004-10.39
42.5	1.6	2.65	108.34	03.03.0004-10.38
42.4	1.6	2.4	113.19	03.03.0004-10.37
42.5	1.6	2.12	110.22	03.03.0004-10.36
42.4	1.6	1.92	107.82	03.03.0004-10.35
42.4	1.6	1.72	108.72	03.03.0004-10.34
42.4	1.6	1.55	106.9	03.03.0004-10.33
42.5	1.7	10.7	116.5	03.03.0004-10.54
42.6	1.7	11.5	115.8	03.03.0004-10.56
42.5	1.7	12.3	119.4	03.03.0004-10.67

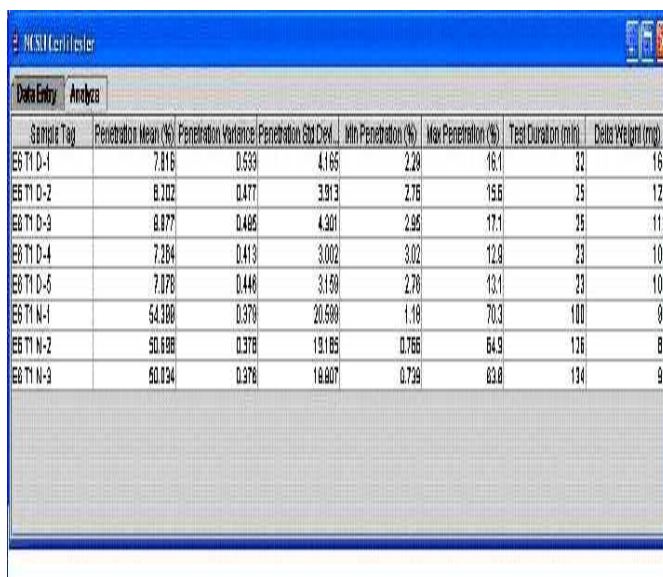
Figure 7.3: Database I/O Window

The sampling procedure:

The generic information about the test sample is initially fed into the database. User starts recording penetration readings using hyper terminal to a file. Once the readings are complete, user enters additional generic information and provides the location of the penetration data to the application and hits load penetration button. The application loads the penetration data into a table. The user then hits save button, at this stage the program generates a unique ID based on the test data and saves the results into the database. The user can also select search to find the corresponding record in the database and load the information to the application.

The penetration information can be plotted by simply selecting the rows and copying them into MS Excel® or another software. The plots can also be analyzed in the database itself and printed. The application provides various capabilities such as zoom, delete etc.

The data acquisition system for data collection was developed by Melih Gunay, PhD student, Fiber and Polymer Science, NCSU.



Sample Tag	Penetration Mean (%)	Penetration Variance	Penetration Std Dev	Min Penetration (%)	Max Penetration (%)	Test Duration (min)	Delta Weight (mg)
E6 T1 D-1	7.816	0.536	4.165	2.28	16.1	22	164
E6 T1 D-2	8.202	0.477	3.913	2.76	15.6	25	122
E6 T1 D-3	8.877	0.485	4.301	2.95	17.1	25	113
E6 T1 D-4	7.284	0.413	3.002	3.02	12.8	23	105
E6 T1 D-5	7.078	0.440	3.150	2.78	13.1	23	100
E6 T1 N-1	54.380	0.378	20.589	1.18	70.3	100	90
E6 T1 N-2	50.898	0.378	19.185	0.765	64.9	126	87
E6 T1 N-3	50.124	0.378	18.807	0.729	63.8	134	91

Figure 7.4: Search Window in the Database

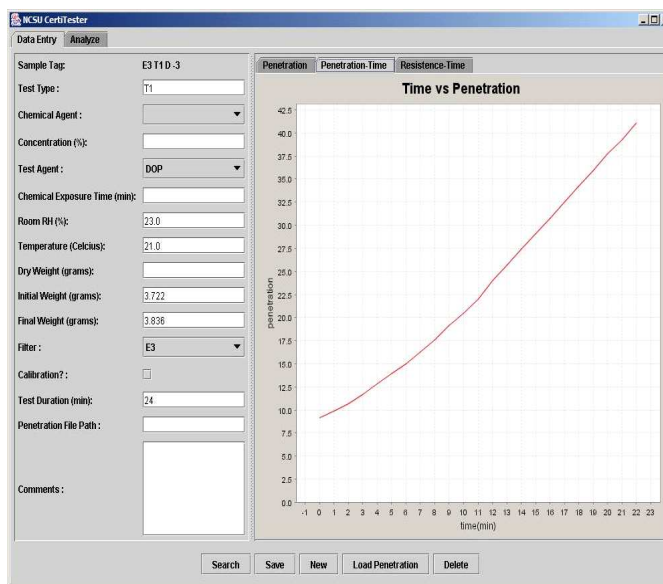


Figure 7.5: Data Assimilation and Analysis

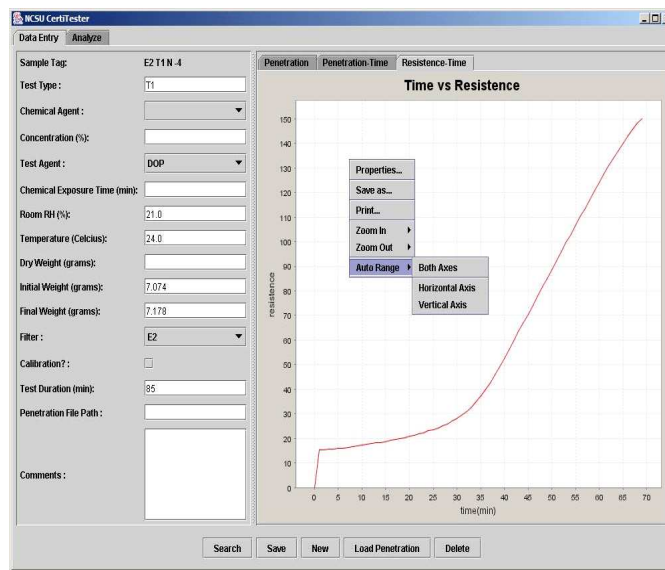


Figure 7.6: Database Capabilities

List of References

- [1] R. Brown, "Electrically charged filter materials," *Engineering Science and Education Journal*, pp. 71–79, April 1992.
- [2] J. Doshi and D. H. Reneker, "Electrospinning process and applications of electrospun fibers," *Journal of Electrostatics*, vol. 35, no. 2-3, pp. 151–160, August 1995.
- [3] P. B. Keady, "Measurement techniques for determining the fractional penetration and MPPS of air filter media," TSI, PO Box 64394, St. Paul MN, Tech. Rep. A 96, March 1995.
- [4] T. Johnson and S. Smith, "Correlation of penetration results between filter testers that use different particle generators and detection methods," in *Technical Report*, St. Paul MN, March 1998.
- [5] D. Walsh and J. Stenhouse, "The effect of particle size, charge, and composition on the loading characteristics of an electrically active fibrous filter material," *Journal of Aerosol Science*, vol. 28, no. 2, pp. 307–321, March 1997.
- [6] D. Walsh and J. Stenhouse, "Clogging of electrically active fibrous filter material," *Powder Technology: experimental results and two-dimensional simulations*, vol. 93, pp. 63–75, 1997.
- [7] D.-H. Han, "Performance of respirator filters using quality factor in Korea," *Industrial Health*, vol. 38, pp. 380–384, 2000.
- [8] R. Brown and D. Wake, "Loading filters with monodisperse aerosols: Macroscopic treatment," *Journal of Aerosol Science*, vol. 30, no. 2, pp. 227–234, February 1999.
- [9] R. Brown, D. Wake, R. Gray, D. Blackford, and G. Bostock, "Effect of industrial aerosols on the performance of electrically charged filter material," *Association of Occupational Hygiene*, vol. 32, no. 3, pp. 271–294, 1988.
- [10] C.-S. Wang, "Electrostatic forces in fibrous filters - a review," *Powder Technology*, vol. 118, no. 1-2, pp. 166–170, August 2001.
- [11] B. Lowkis and E. Motyl, "Electret properties of polypropylene fabrics," *Journal of electrostatics*, vol. 51-52, pp. 232–238, 2001.

-
- [12] R. Brown, *Air Filtration: An Integrated Approach to the Theory and Applications of Fibrous Filters*. New York, NY: Pergamon Press Inc., 1993.
- [13] L. Barrett and A. Rousseau, "Aerosol loading performance of electret filter media," *American Industrial Hygiene Association Journal*, vol. 59, pp. 532–539, 1998.
- [14] W. H. Revoir and C.-T. Bien, *Respiratory Protection Handbook*. Florida: Lewis Publishers, Inc, February 1997.
- [15] P. Smith, G. East, R. Brown, and D. Wake, "Generation of triboelectric charge in textile fibre mixtures, and their use in air filters," *Journal of Electrostatics*, vol. 21, no. 1, pp. 81–98, July 1988.
- [16] G. Sessler, "Electrets: Recent developments," *Journal of Electrostatics*, vol. 51-52, pp. 137–145, May 2001.
- [17] P. P. Tsai, H. Schreuder-Gibson, and P. Gibson, "Different electrostatic methods for making electret filters," *Journal of Electrostatics*, vol. 54, no. 3-4, pp. 333–341, March 2002.
- [18] C. Chen and S. Huang, "The effects of particle charge on the performance of a filtering face-piece," *American Industrial Hygiene Association Journal*, vol. 59, pp. 227–233, April 1998.
- [19] F. Romay, B. Liu, and S. Chae, "Experimental study of electrostatic capture mechanisms in commercial electret filters," *Aerosol Science and Technology*, vol. 28, no. 3, pp. 224–234, March 1998.
- [20] R. Lathrache and H. Fissan, "Fractional penetrations for electrostatically charged fibrous filter in the submicron particle size range," *Particle Characterization*, vol. 3, no. 2, pp. 74–80, 1986.
- [21] F. Romay, B. Liu, and S. Chae, "Electrostatic particle capture in commercial electret filters," in *Proceedings of the 1997 National Technical Conference of the American Filtration and Separations Society*, Minneapolis, MN, April 29 - May 2 1997.
- [22] F. Romay, B. Liu, and S. Chae, "Degradation of electret filters during DOP aerosol loading," in *Proceedings of the 1998 National Technical Conference of the American Filtration and Separations Society*, St. Louis, MO, May 4-7 1998.
- [23] R. Brown, J. Davies, and D. Wake, "Penetration of test aerosols through filters described in terms of a gamma distribution of layer efficiencies," *Journal of Aerosol Science*, vol. 18, no. 5, pp. 499–509, October 1987.
- [24] J. Ji, G. Bae, S. Kang, and J. Hwang, "Effect of particle loading on the collection performance of an electret cabin air filter for submicron aerosols," *Journal of Aerosol Science*, vol. 34, no. 11, pp. 1493–1504, November 2003.
-

-
- [25] R. Brown, "Capture of dust particles in filters by line-dipole charged fibers," *Journal of Aerosol Science*, vol. 12, no. 4, pp. 349–356, 1981.
- [26] D. Walsh and J. Stenhouse, "Parameters affecting the loading behavior and degradation of electrically active filter materials," *Aerosol Science and Technology*, vol. 29, no. 5, pp. 419–432, November 1998.
- [27] H. Baumgartner and F. Löffler, "The collection performance of electret filters in the particle size range 10 nm - 10 μm ," *Journal of Aerosol Science*, vol. 17, no. 3, pp. 438–445, 1986.
- [28] E. S. Moyer and M. Bergman, "Electrostatic N-95 respirator filter media efficiency degradation resulting from intermittent sodium chloride aerosol exposure," *Applied Occupational and Environmental Hygiene*, vol. 15, no. 8, pp. 600–608, 2000.
- [29] Y. Otani, H. Emi, and J. Mori, "Initial collection efficiency of electret filter and its durability for solid and liquid particles," *KONA Powder and Particle*, vol. 11, pp. 207–214, 1993.
- [30] D. L. Myers and B. D. Arnold, "Mechano-electret filtration media: Synergy of structure and electrostatic charge," *Filtration and Separation*, vol. 40, no. 5, pp. 24–27, June 2003.
- [31] A. H. Biermann, B. Lum, and W. Bergman, "Evaluation of permanently charged electrofibrous filters," in *Proceedings of the 17th Department of Energy Nuclear Air Cleaning Conference Denver CO*. Livermore CA: Lawrence Livermore National Laboratory, 1982.
- [32] Q. Chen, "Investigation of corona charge stability mechanisms in polytetrafluoroethylene(ptfe) teflon films after plasma treatment," *Journal of Electrostatics*, vol. 59, pp. 3–13, 2003.